

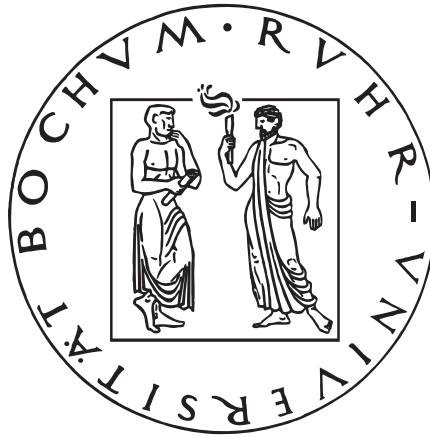
Meson loops in the Nambu–Jona-Lasinio model

Emil N. Nikolov^a, Wojciech Broniowski^b, Christo V. Christov^a,
Georges Ripka^c, and Klaus Goeke^a

^a *Institut für Theoretische Physik II, Ruhr-Universität Bochum,
D-44780 Bochum, Germany*

^b *H. Niewodniczański Institute of Nuclear Physics, PL-31342 Cracow, Poland*

^c *Service de Physique Théorique, Centre d'Etudes de Saclay, F-91191
Gif-sur-Yvette Cedex, France*



Ruhr-Universität Bochum
Institut für Theoretische Physik II
Teilchen- und Kernphysik

Meson loops in the Nambu-Jona-Lasinio model

Emil N. Nikolov ^{a,1}, Wojciech Broniowski ^b,
Christo V. Christov ^{a,1}, Georges Ripka ^c, and Klaus Goeke ^a

^a*Institut für Theoretische Physik II, Ruhr-Universität Bochum,
D-44780 Bochum, Germany*

^b*H. Niewodniczański Institute of Nuclear Physics, PL-31342 Cracow, Poland*

^c*Service de Physique Théorique de Saclay, F-91191 Gif-sur-Yvette Cedex, France*

Abstract

We calculate the effects of meson loops in the vacuum sector of the Nambu–Jona-Lasinio model. Using the effective action formalism we take consistently all next-to-leading-order $\frac{1}{N_c}$ terms into account. This leads to a symmetry-conserving approach, in which all features of spontaneously broken chiral symmetry, such as the Goldstone theorem, the Goldberger–Treiman and the Gell-Mann–Oakes–Renner relations are preserved. Contributions to $\langle \bar{q}q \rangle$ and F_π are calculated, and are shown to be substantial, at the level of $\sim 30\%$, consistent with the $\frac{1}{N_c}$ expansion.

PACS numbers: 12.39.-x, 12.39.Fe, 14.40.-n

1 Introduction

Over the last few years the Nambu–Jona-Lasinio model [1] has been used extensively to study numerous features of strong-interaction physics at low energies (for recent reviews on mesons see [2–4], and on baryons see [5,6]). The four-fermion point interaction leads to dynamical chiral symmetry breaking

¹ On leave of absence from Institute for Nuclear Research and Nuclear Energy, 1784 Sofia, Bulgaria

² E-mail: emiln *or* christoc *or* goeke@hadron.tp2.ruhr-uni-bochum.de
wojtek@humboldt.ifj.edu.pl
ripka@amoco.saclay.cea.fr

which plays a key role for the description of low-energy hadron phenomena. An attractive feature of the model is that having a small number of free parameters it allows for a unified description of mesons and baryons, with both two and three flavors. The resulting hadron spectroscopy has been quite successful: the basic mass relations, the electromagnetic form factors and the electromagnetic polarizabilities are reproduced reasonably well.

All the above applications have been performed in the *one quark-loop* approximation. The effective action, the meson and quark self-energies, vertex functions, *etc.*, are all generated by a quark-loop. This approximation is justified by the large- N_c limit, in which meson loops are $\frac{1}{N_c}$ -suppressed. However, meson loops cannot always be neglected since in the real world $N_c = 3$. More importantly, the pions are very light, and in many situations pionic effects, although formally $\frac{1}{N_c}$ -suppressed, are enhanced because of the low pion mass. For example, pionic thermal excitations described by meson loops are dominating in hadronic systems at finite temperature. Meson loops are also required for the proper description of heavier mesons. For example, the σ or the ρ mesons can split into two pions and this effect is again described by pionic loops [7,8].

There have been a number of attempts [9–12] to include meson loops in the Nambu–Jona-Lasinio model. These approaches are based on $\frac{1}{N_c}$ expansion in terms of Feynman graphs. The symmetry properties of the system, however, can be easily violated by an inappropriate choice of diagrams. This is the case of Refs. [9–11] where basic symmetry relations, such as *e.g.* the Goldstone theorem, are violated. The reason for this is that the gap equation and the meson propagators are not treated consistently. We show that in order to guarantee the validity of the Goldstone theorem on the basis of a consistent $\frac{1}{N_c}$ expansion it is crucial to determine both the constituent quark mass and the meson propagators consistently from the effective action including one meson loop. Methods which preserve the symmetry properties at higher orders are called *symmetry-conserving approximations* [13,14]. The approach of Ref. [12] is up to our knowledge the only one which preserves the Goldstone theorem at the one meson-loop level. This is achieved by a judicious choice of Feynman diagrams.

In this paper we extend consistently the Nambu–Jona-Lasinio model to next-to-leading order in $\frac{1}{N_c}$ which includes the meson-loop contributions. We use the effective action formalism which leads in a natural way to a symmetry conserving approximation. Our approach identifies the Feynman diagrams which need to be included to maintain the symmetry properties, at any level of approximation. In our calculation the pion remains massless in the chiral limit and the basic relations following from Ward-Takahashi identities, such as the Gell-Mann–Oaks–Renner relation and the Goldberger-Treiman relation are satisfied. We calculate contributions of meson loops to the quark condensate $\langle \bar{q}q \rangle$, and to the pion decay constant F_π , and find them to be substantial, of the order of 30%. This is consistent with the N_c -counting scheme.

2 The effective action

We use the simplest version of the $SU(2)$ Nambu–Jona-Lasinio model with scalar and pseudoscalar couplings only. The Lagrangian of the model is given by

$$\mathcal{L} = \bar{q}(i\partial^\mu\gamma_\mu - m)q + \frac{G}{2} \left((\bar{q}q)^2 + (\bar{q}i\gamma_5\vec{\tau}q)^2 \right), \quad (1)$$

where the point-like four-quark interaction is characterized by the coupling constant G with the dimension of inverse energy squared, q stands for up and down quarks with $N_c = 3$ colors, and m is the current quark mass. The partition function of the system is given by the path integral

$$Z \equiv e^{-W} = \int \mathcal{D}q^\dagger \mathcal{D}q e^{-\mathcal{I}(q^\dagger, q)}. \quad (2)$$

The integration is over the Grassmann variables q^\dagger and q , and $\mathcal{I}(q^\dagger, q)$ is the Euclidean action

$$\mathcal{I}(q^\dagger, q) = \int d^4x q^\dagger \left(\partial_\tau - i\vec{\alpha} \cdot \vec{\nabla} + \beta m \right) q - \frac{G}{2} \left((q^\dagger \beta q)^2 + (q^\dagger i\beta \gamma_5 \vec{\tau} q)^2 \right). \quad (3)$$

The partially bosonized version of the model [15] is obtained by introducing auxiliary meson fields Φ . At this stage we also introduce mesonic sources χ , and get

$$Z(\chi) = \int \mathcal{D}q^\dagger \mathcal{D}q \mathcal{D}\Phi \exp \left\{ - \int d^4x \left[q^\dagger \left(\partial_\tau - i\vec{\alpha} \cdot \vec{\nabla} + \beta \Gamma_\alpha \Phi_\alpha \right) q + \frac{1}{2} a^2 \Phi^2 - a^2 m \Phi_0 - \chi_\alpha \Phi_\alpha \right] \right\}, \quad (4)$$

where we use the following notation

$$\begin{aligned} a^2 &= G^{-1}, \\ \Gamma_0 &= 1; \quad \Gamma_\alpha = i\gamma_5 \tau_\alpha, \quad \alpha = 1, 2, 3, \\ \Phi_0 &= S; \quad \Phi_\alpha = P_\alpha, \quad \alpha = 1, 2, 3. \end{aligned} \quad (5)$$

We have omitted the term $\frac{1}{2}a^2m^2$ in the exponent of Eq. (4) since it is a constant independent of the fields. The quark fields, which appear in the exponent of Eq. (4) in a quadratic form, can be integrated out, and the partition function becomes

$$Z(\chi) \equiv e^{-W(\chi)} = \int \mathcal{D}\Phi e^{-I(\Phi, \chi)}, \quad (6)$$

where $\int \mathcal{D}\Phi \equiv \int \mathcal{D}S\mathcal{D}\vec{P}$, and $W(\chi)$ is the generating functional of the connected field propagators. The *bosonized* Euclidean action $I(\Phi, \chi)$ is

$$I(\Phi, \chi) = -N_c \text{Tr} \ln D + \frac{a^2}{2} \int d^4x \Phi^2 - a^2 m \int d^4x \Phi_0 - \int d^4x \chi_\alpha \Phi_\alpha. \quad (7)$$

The Dirac operator is

$$D = \partial_\tau + h \quad (8)$$

with the one-particle Dirac Hamiltonian h given by

$$h = -i\vec{\alpha} \cdot \vec{\nabla} + \beta \Gamma_\alpha \Phi_\alpha. \quad (9)$$

The trace in Eq. (7) involves an integration over space-time variables and a matrix trace over the spin and flavor degrees of freedom. The trace over color gives a factor N_c which we write explicitly. Recalling that the quark propagator in the background meson fields Φ is given by D^{-1} , we refer to the term $N_c \text{Tr} \ln D$ as to the *quark-loop contribution*.

For simplicity we use the following notation throughout the paper: the indices a, b, \dots contain the field isospin indices α, β, \dots and the space-time coordinates x_a, x_b, \dots , *i.e.* $a \equiv \{\alpha, x_a\}$, $b \equiv \{\beta, x_b\}$, *etc.* Summation/integration over repeated indices is understood.

Generally, the quark-loop contribution $N_c \text{Tr} \ln D$ can have an imaginary part which is related to the *anomalous* terms. In the case of SU(2) with scalar and pseudoscalar mesons this imaginary part vanishes identically and the one quark-loop contribution is given by the real part: $N_c \text{Tr} \ln D = \frac{1}{2} N_c \text{Tr} \ln(D^\dagger D)$ so that the Euclidean action, with sources χ , can also be written in the form

$$I(\Phi, \chi) = -\frac{1}{2} N_c \text{Tr} \ln(D^\dagger D) + \frac{a^2}{2} \Phi^2 - a^2 m \Phi_0 - \chi_a \Phi_a. \quad (10)$$

The expectation value of the field Φ and the connected meson Green's functions are given by

$$\begin{aligned} \langle \Phi_a \rangle &= - \left. \frac{\delta W(\chi)}{\delta \chi_a} \right|_{\chi=0}, \\ K_{ab} &= - \left. \frac{\delta^2 W(\chi)}{\delta \chi_a \delta \chi_b} \right|_{\chi=0} = \langle T[\Phi_a, \Phi_b] \rangle - \langle \Phi_a \rangle \langle \Phi_b \rangle. \end{aligned} \quad (11)$$

The *effective action* $\Gamma(\Phi)$ is defined through the Legendre transformation [16,17,14]

$$\Gamma(\Phi) = W(\chi) + \chi_a \Phi_a, \quad \Phi_a(\chi) = - \frac{\delta}{\delta \chi_a} W(\chi), \quad (12)$$

where we apply the common convention of using the same symbol for the field Φ_a and its expectation value $\langle \Phi_a \rangle$. It is straightforward to deduce that the effective action $\Gamma(\Phi)$ is stationary with respect to variations of the (expectation values of the) fields, and that the *inverse* field propagators (11) can be calculated as the second variation of the effective action $\Gamma(\Phi)$ with respect to the fields Φ *taken at the stationary point* Φ^{st} of the effective action

$$\left. \frac{\delta \Gamma(\Phi)}{\delta \Phi_a} \right|_{\Phi^{\text{st}}} = 0, \quad K_{ab}^{-1} = \left. \frac{\delta^2 \Gamma(\Phi)}{\delta \Phi_a \delta \Phi_b} \right|_{\Phi^{\text{st}}}. \quad (13)$$

Successive approximations to the path integral (6) lead to successive approximations to the effective action $\Gamma(\Phi)$. In order to evaluate the path integral we expand the action $I(\Phi, \chi)$ around its stationary point $\tilde{\Phi}(\chi)$, which is given by:

$$\left. \frac{\delta I(\Phi, \chi)}{\delta \Phi_a} \right|_{\tilde{\Phi}(\chi)} = 0. \quad (14)$$

Taking only the leading order term, $I(\tilde{\Phi}, \chi)$, in this expansion we obtain the generating functional in the leading- N_c or saddle-point approximation

$$Z(\chi) = e^{-I(\tilde{\Phi}, \chi)}. \quad (15)$$

In this approximation the effective action includes only one quark-loop contributions and no meson loops.

Let us now consider fluctuations of the meson fields about the stationary fields. Denoting the meson-field fluctuations by

$$\phi = \Phi - \tilde{\Phi} \quad (16)$$

and taking the terms up to second order in ϕ in the expansion of the action we obtain for the generating functional (4)

$$Z(\chi) = e^{-I(\tilde{\Phi}, \chi)} \int \mathcal{D}\phi e^{-\frac{1}{2} \phi_a \left(\left. \frac{\delta^2 I(\Phi)}{\delta \Phi_a \delta \Phi_b} \right|_{\tilde{\Phi}} \right) \phi_b}. \quad (17)$$

We can now take the path integral over ϕ which leads to the following generating functional

$$W(\chi) = I(\tilde{\Phi}) - \chi_a \tilde{\Phi}_a + \frac{1}{2} \text{Tr} \ln \left. \frac{\delta^2 I(\Phi)}{\delta \Phi \delta \Phi} \right|_{\tilde{\Phi}(\chi)}, \quad (18)$$

where the last term originating from the integral over the fluctuations of the meson fields is the meson-loop contribution. The corresponding effective action

is

$$\Gamma(\Phi) = I(\tilde{\Phi}) - \chi_a \tilde{\Phi}_a + \chi_a \Phi_a + \frac{1}{2} \text{Tr} \ln \frac{\delta^2 I(\Phi)}{\delta \Phi \delta \Phi} \Big|_{\tilde{\Phi}(\chi)}. \quad (19)$$

The first term in (18) is leading order ($\mathcal{O}(N_c)$), and the last term is next to leading order ($\mathcal{O}(N_c^0)$). Thus, according to (12), the difference $\phi = \Phi - \tilde{\Phi}$ is suppressed by $\frac{1}{N_c}$ related to Φ . Since the effective action $I(\tilde{\Phi}, \chi)$ is stationary at $\tilde{\Phi}$, we have

$$I(\Phi, \chi) - I(\tilde{\Phi}, \chi) = \frac{1}{2} \phi_a \left(\frac{\delta^2 I(\Phi)}{\delta \Phi_a \delta \Phi_b} \Big|_{\tilde{\Phi}} \right) \phi_b \sim \mathcal{O} \left(\frac{1}{N_c} \right). \quad (20)$$

We neglect this difference since it is $\frac{1}{N_c}$ -suppressed compared to the next-to-leading order term, and of order $\frac{1}{N_c^2}$ related to the leading order. This gives the effective action

$$\Gamma(\Phi) = I(\Phi) + \frac{1}{2} \text{Tr} \ln \frac{\delta^2 I(\Phi)}{\delta \Phi \delta \Phi}. \quad (21)$$

The same result can also be deduced by a resummation of Feynman graphs, in terms of quark propagators which are dressed by a general static potential [14,18]. We refer to the effective action given by the leading order term $I(\Phi)$ as the one quark-loop approximation, and to the action (21), including both the leading and next to leading order term $\frac{1}{2} \text{Tr} \ln \frac{\delta^2 I(\Phi)}{\delta \Phi \delta \Phi}$, as the one meson-loop approximation. We emphasize that in our approach they are both symmetry conserving approximations.

3 The one quark-loop approximation

We first consider the one quark-loop approximation, in which the effective action $\Gamma(\Phi)$ has the same form as the action (10) in the absence of sources

$$\Gamma(\Phi) = I(\Phi) = -\frac{N_c}{2} \text{Tr} \ln(D^\dagger D) + \frac{a^2}{2} \Phi^2 - a^2 m \Phi_0. \quad (22)$$

The effective action (22) is ultraviolet divergent and requires regularization. To this aim a fermion-loop cut-off Λ_f is introduced. Since the model is non-renormalizable, the cut-off Λ_f is kept finite and treated as a parameter. The other two model parameters are the coupling constant $G = \frac{1}{a^2}$ and the current quark mass m . If we fit the pion mass and the pion decay constant, we are left with only one free parameter.

In this paper we use two regularization schemes, namely the proper-time regularization and the covariant four-momentum $O(4)$ regularization, as used in Ref. [19]. We will compare results obtained with these schemes. The proper-time regularized effective action is given by

$$\Gamma_{\Lambda}(\Phi) = I_{\Lambda}(\Phi) = \frac{N_c}{2} \text{Tr} \int_{\Lambda_f^{-2}}^{\infty} \frac{ds}{s} e^{-sD^{\dagger}D} + \frac{a^2}{2} \Phi^2 - a^2 m \Phi_0. \quad (23)$$

In the $O(4)$ regularization, the four-momentum running in the quark loop is limited by $|k| < \Lambda_f$ as explained in App. C.2. In the following we will always use the regularized action and skip the index Λ . The action (23) has a translationally invariant stationary point at $\Phi = \bar{\Phi}$

$$\left. \frac{\delta I(\Phi)}{\delta \Phi_a} \right|_{\bar{\Phi}} = 0, \quad \bar{\Phi} = \{M_0, \vec{P} = 0\} \quad (24)$$

which is identified with the vacuum. At the one quark-loop level the stationary field configuration coincides with the expectation value of the meson field: $\bar{\Phi} = \langle \Phi \rangle$. Inserting the regularized effective action (23) into Eq.(24) we get the following equation for M_0

$$a^2 \left(1 - \frac{m}{M_0} \right) - 8N_c g(M_0) = 0, \quad (25)$$

where the function $g(S)$ is defined in App. C. Equation (25) is commonly referred to as the gap equation since it determines the energy gap $2M_0$ between the negative- and positive-energy quark states.

The inverse meson propagators (13) are given by the second variation of the action with respect to the fields, taken *at the stationary point* $\Phi = \bar{\Phi}$

$$K_{ab} = \left(\left. \frac{\delta^2 I(\Phi)}{\delta \Phi \delta \Phi} \right|_{\bar{\Phi}} \right)_{ab}^{-1}. \quad (26)$$

In momentum space the meson propagators are given by [19]

$$K_{\alpha\beta}(q^2) = \delta_{\alpha\beta} \left\{ 4N_c \left(f(M_0, q^2)(q^2 + 4M_0^2 \delta_{\alpha 0}) - 2g(M_0) \right) + a^2 \right\}^{-1}, \quad (27)$$

where the function $f(S, q^2)$ describing a quark loop with two meson couplings is given in App. C. Since we are evaluating the propagator at the stationary point $\bar{\Phi}$, we can use the gap equation (25) in order to simplify this expression and we obtain the pseudoscalar and scalar field propagators in the form

$$K_\pi(q^2) = \left\{ 4N_c f(M_0, q^2) q^2 + a^2 \frac{m}{M_0} \right\}^{-1}, \quad (28)$$

$$K_\sigma(q^2) = \left\{ 4N_c f(M_0, q^2) (q^2 + 4M_0^2) + a^2 \frac{m}{M_0} \right\}^{-1}. \quad (29)$$

The propagators have poles at $q^2 = -m_\phi^2$

$$m_\pi^2 = \frac{a^2 m}{4N_c f(M_0, q^2 = -m_\pi^2) M_0}, \quad (30)$$

$$m_\sigma^2 = 4M_0^2 + \frac{a^2 m}{4N_c f(M_0, q^2 = -m_\sigma^2) M_0}, \quad (31)$$

where m_π and m_σ are the on-shell pion and σ -meson masses. In the chiral limit ($m \rightarrow 0$), the pseudoscalar mesons are massless Goldstone bosons, as expected. The physical quark-meson coupling constant $g_{\pi qq}$ is given by the residue at the pole of the pion propagator

$$g_{\pi qq}^2 = \lim_{q^2 \rightarrow -m_\pi^2} (q^2 + m_\pi^2) K_\pi(q^2), \quad (32)$$

which gives in the chiral limit

$$g_{\pi qq} = (4N_c f(M_0, 0))^{-\frac{1}{2}}. \quad (33)$$

To end of this section we recall the N_c -counting rules for quark and meson loops in the Nambu–Jona-Lasinio model. From the gap equation (25) it follows that the coupling constant $G = \frac{1}{a^2}$ must be considered proportional to $\frac{1}{N_c}$. Each quark-loop contributes a factor of N_c , which comes from the trace over color degrees of freedom. For example, the action $I(\Phi)$ is of order N_c due to the term $N_c \text{Tr} \ln D$. The meson propagators (26) contain a quark-loop in the denominator and are hence of order $\frac{1}{N_c}$, as can be seen directly from Eq. (27). From Eq. (33) we see that the physical pion-quark coupling constant $g_{\pi qq}$ is of order $N_c^{-\frac{1}{2}}$. The physical meson propagators are obtained by rescaling the meson fields by the factor $g_{\pi qq}$. This leads to the propagators for the physical meson fields ($\phi = \Phi/g_{\pi qq}$) of the form $K_{\alpha\beta}(q^2)/g_{\pi qq}^2$ which are of order N_c^0 . For each quark-meson vertex we have a factor of $g_{\pi qq} \sim N_c^{-\frac{1}{2}}$. This way, our N_c -counting rules agree with those of QCD [20,21].

4 The effective action including one meson loop

In this section we include the meson-loop contribution to the effective potential, which is the second term of the expression (21). This leads to corrections

which are next-to-leading order in N_c . We now consider the effective action in the form

$$\Gamma(\Phi) = I(\Phi) + \frac{1}{2} \text{Tr} \ln K^{-1}(\Phi), \quad (34)$$

where $K^{-1}(\Phi)$ is the functional

$$K_{ab}^{-1}(\Phi) \equiv \frac{\delta^2 I(\Phi)}{\delta \Phi_a \delta \Phi_b}. \quad (35)$$

Evaluating the meson-loop term, $\frac{1}{2} \text{Tr} \ln K^{-1}(\Phi)$, we encounter new divergences which arise due to the integration over the momentum in the meson-loop. Let us analyze the meson-loop momentum integrals from a formal point of view. In our model, which has only quark dynamical degrees of freedom, the meson propagator at the leading N_c -level is given by a chain of quark-loops. We have regularized the quark-loop contribution introducing a fermionic cut-off parameter Λ_f . This regularization, however, does not restrict the four-momenta of the mesons. Using the asymptotics of the function $f(S, q^2)$ at high momenta it can be easily shown that the leading order field propagator has the asymptotic expansion $K_{\alpha\beta}^{-1}(q^2) \approx \delta_{\alpha\beta} a^2 + \mathcal{O}\left(\frac{1}{q^2}\right)$. Thus, integrating over the meson-loop four-momentum in (34) we encounter a quartic divergence. Similarly, calculating the pion propagator at the one meson-loop level we will obtain both quadratically and logarithmically divergent terms. We regularize the meson-loop integrals introducing a new *bosonic* cut-off parameter Λ_b . We use a covariant $O(4)$ regularization for the meson loop, consisting in cutting off the meson four-momenta in the loop integrals at $Q^2 = \Lambda_b^2$. This is the simplest possible choice.

The one meson-loop effective action (34) has a translationally invariant stationary point given by the equation

$$\left. \frac{\delta \Gamma(\Phi)}{\delta \Phi_a} \right|_{\bar{\Phi}} = 0, \quad \bar{\Phi} = \{M, \vec{P} = 0\}. \quad (36)$$

The stationary point of the one meson-loop effective action Γ is denoted by $\bar{\bar{\Phi}}$, in order to distinguish it from the stationary point $\bar{\Phi}$ of the quark-loop action defined in Eq. (24). Variation of the effective action (34) with respect to the meson fields leads to the stationary-point condition (36) in the form of a generalized gap equation:

$$\left. \frac{\delta \Gamma(\Phi)}{\delta \Phi_a} \right|_{\bar{\bar{\Phi}}} = S_a(\bar{\bar{\Phi}}) + \frac{1}{2} S_{abc}(\bar{\bar{\Phi}}) K_{bc}(\bar{\bar{\Phi}}) = 0, \quad (37)$$

where we have introduced the following short-hand notation for the n -leg quark-loop meson vertices

$$S_{a_1 a_2 \dots a_n}(\overline{\overline{\Phi}}) \equiv \frac{\delta^n I(\Phi)}{\delta \Phi_{a_1} \delta \Phi_{a_2} \dots \delta \Phi_{a_n}} \Big|_{\overline{\overline{\Phi}}} . \quad (38)$$

For $a = 1, 2, 3$, the condition (37) is trivially satisfied with a vanishing pion field. From the variation over the sigma field we obtain

$$S_0(\overline{\overline{\Phi}}) + \frac{1}{2} S_{0bc}(\overline{\overline{\Phi}}) K_{bc}(\overline{\overline{\Phi}}) = 0 . \quad (39)$$

The diagrams contributing to this equation are shown in Fig. 1. Using the N_c -counting rules (see Section 3) it can be verified that the meson-loop diagram (b) is of order N_c^0 and hence by one power in $\frac{1}{N_c}$ suppressed compared to the quark-loop diagram, which is of order N_c .

The leading-order meson propagators in Eq. (39) $K_{bc}(\overline{\overline{\Phi}})$ are evaluated at the stationary point of the one meson loop effective action $\overline{\overline{\Phi}}$. In momentum space, similarly to Eq. (27), we obtain

$$\begin{aligned} K_{\alpha\beta}^{-1}(M, q^2) &= \delta_{\alpha\beta} \left\{ 4N_c \left(f(M, q^2)(q^2 + 4M^2 \delta_{\alpha 0}) - 2g(M) \right) + a^2 \right\} \\ &= \widetilde{K}_{\alpha\beta}^{-1}(M, q^2) + \delta_{\alpha\beta} \Delta(M) , \end{aligned} \quad (40)$$

where we have defined

$$\widetilde{K}_{\alpha\beta}^{-1}(M, q^2) = \delta_{\alpha\beta} 4N_c f(M, q^2)(q^2 + 4M^2 \delta_{\alpha 0}) \quad (41)$$

and

$$\Delta(M) = -8N_c g(M) + a^2 . \quad (42)$$

Since $\Delta(M)$ is exactly equal to the first term $S_0(\overline{\overline{\Phi}})$ in the gap equation (39) we have

$$\Delta(M) = S_0(\overline{\overline{\Phi}}) = -\frac{1}{2} S_{0bc}(\overline{\overline{\Phi}}) K_{bc}(\overline{\overline{\Phi}}) = \mathcal{O}(N_c^0) , \quad (43)$$

which shows that $\Delta(M)$ is one order in N_c suppressed compared to the full propagators (40) which are of order N_c . Inserting the decomposition (40) into the gap equation (39) we obtain

$$S_0(\overline{\overline{\Phi}}) + \frac{1}{2} S_{0bc}(\overline{\overline{\Phi}}) \widetilde{K}_{bc}(\overline{\overline{\Phi}}) - \frac{1}{2} S_{0bc}(\overline{\overline{\Phi}}) \widetilde{K}_{bd}(\overline{\overline{\Phi}}) S_0(\overline{\overline{\Phi}}) \widetilde{K}_{dc}(\overline{\overline{\Phi}}) + \dots = 0 . \quad (44)$$

The third term in this expansion is of order $\frac{1}{N_c}$ and hence one order in N_c suppressed compared to the meson-loop contribution (the second term). Further terms are suppressed by even higher powers of N_c . We therefore keep only the first two terms in the gap equation (44). This is a crucial point of our approach. If we did not maintain this consistency in N_c -counting, we would encounter another problem, namely the appearance of negative eigenvalues of $K^{-1}(\Phi)$ at low momenta for $M < M_0$. We would then be unable to calculate the effective potential (34).

The meson-loop diagram (Fig. 1(b)) is evaluated in App. B.1. The contribution of the quark-loop diagram (Fig. 1(a)) is given by the lhs of the one quark-loop gap equation (25), with the constituent quark mass M_0 replaced by M . Finally, adding up all contributions from App. B.1 we obtain the explicit form of the one meson-loop gap equation:

$$a^2 \left(1 - \frac{m}{M}\right) - 8N_c g(M) + N_c \frac{1}{4\pi^2} \int_0^{\Lambda_b^2} d(Q^2) Q^2 \left\{ 4f(M, Q^2) \widetilde{K}_{00}(M, Q^2) + \sum_{\beta\gamma} \left(2f(M, 0) - f_1(M, Q^2)(Q^2 + 4M^2\delta_{\beta 0})\right) \widetilde{K}_{\beta\gamma}(M, Q^2) \right\} = 0. \quad (45)$$

The functions f , f_1 and g are defined in App. C. The position of the minimum M of the one meson-loop effective action determines the energy gap in the spectrum for the constituent quarks and analogously to the one quark-loop case we refer to it as the constituent quark mass (in the one meson-loop approximation).

5 Quark condensate

In the effective action formalism the quark condensate $\langle \bar{q}q \rangle$ is given by

$$\langle \bar{q}q \rangle = \frac{\delta \Gamma(\Phi)}{\delta m}. \quad (46)$$

Note that since now we are interested in the variation with respect to the current quark mass m we have to take into account the term $\frac{1}{2}a^2m^2$, which we have neglected performing the bosonization (see the comment following Eq. (5)). Adding this term to $I(\Phi)$ in Eq. (34) and performing the variation we obtain

$$\langle \bar{q}q \rangle = -a^2(M - m). \quad (47)$$

Hence, in the chiral limit, the quark condensate is proportional to the constituent quark mass, and it vanishes if the chiral symmetry is not sponta-

neously broken. Comparing the result (47) with the corresponding expression at the one quark-loop level

$$\langle \bar{q}q \rangle = -a^2(M_0 - m), \quad (48)$$

we can see that it is fully analogous, with the constituent quark mass M_0 replaced by M . We shall compare our theoretical results to the empirical value [22]

$$\langle \bar{u}u \rangle = \langle \bar{d}d \rangle = \frac{1}{2} \langle \bar{q}q \rangle = -((250 \pm 50) \text{ MeV})^3. \quad (49)$$

6 Meson propagators

The inverse meson propagators, including the one meson-loop effects, are equal to the second order variation of the effective action (34) with respect to the fields taken at the stationary point $\bar{\bar{\Phi}}$. We obtain the meson field propagators in one meson-loop approximation

$$L_{ab} = \left(\frac{\delta^2 \Gamma(\Phi)}{\delta \Phi \delta \Phi} \bigg|_{\bar{\bar{\Phi}}} \right)_{ab}^{-1}. \quad (50)$$

Performing the variation in (50) we can express the propagators in one meson-loop approximation in terms of the functional $K(\Phi)$ (35) and the quark-loop meson vertices (38)

$$\begin{aligned} L_{ab}^{-1} = & K_{ab}^{-1}(\bar{\bar{\Phi}}) - \frac{1}{2} S_{ace}(\bar{\bar{\Phi}}) K_{cd}(\bar{\bar{\Phi}}) K_{ef}(\bar{\bar{\Phi}}) S_{dfb}(\bar{\bar{\Phi}}) \\ & + \frac{1}{2} S_{abcd}(\bar{\bar{\Phi}}) K_{cd}(\bar{\bar{\Phi}}). \end{aligned} \quad (51)$$

The diagrammatic representation of this equation is shown in Fig. 2. The first term (a) is the leading-order (quark-loop) contribution $K^{-1}(\bar{\bar{\Phi}})$. We have to bare in mind, however, that here it differs from the inverse propagator $K^{-1}(\bar{\Phi})$ (26) since now it is calculated at the stationary point $\bar{\bar{\Phi}}$ of the one meson-loop effective action. This means that the quark propagators appearing in the meson propagator $K(\bar{\bar{\Phi}})$ are dressed by solving the one meson-loop gap equation and have a constituent quark mass M . The second (b) and third term (c) are the one meson-loop contributions to the inverse meson propagator. The dashed lines in the loops can correspond to a pion or to a sigma meson. The one meson-loop contributions are suppressed one order in N_c , which can be easily shown using the N_c -counting rules.

In Eq. (51) $\bar{\bar{\Phi}}$ is the solution of the gap equation (44), in which only the first two terms are retained, so as to be consistent with N_c -counting. It is crucial

to maintain the same N_c -counting consistency in the calculation of the meson propagator (51). Otherwise the pion would not appear as a Goldstone boson. We include in the inverse propagator L^{-1} contributions which are of order N_c and N_c^0 . In the first term K^{-1} , which is defined in Eq. (40), we keep both the contributions \widetilde{K}^{-1} , of order N_c , and the contribution $\Delta(M)$, of order N_c^0 . In the remaining (meson-loop) terms of Eq. (51), the vertices S are of order N_c (because they contain a quark loop) and the leading order of the K factors is N_c^{-1} . Therefore N_c -counting consistency requires the substitution of the K factors by \widetilde{K} factors in the two meson-loop terms. Keeping all terms to order N_c^0 we obtain thus the inverse meson propagators in the form

$$L_{ab}^{-1} = K_{ab}^{-1}(\overline{\Phi}) - \frac{1}{2} S_{ace}(\overline{\Phi}) \widetilde{K}_{cd}(\overline{\Phi}) \widetilde{K}_{ef}(\overline{\Phi}) S_{dfb}(\overline{\Phi}) + \frac{1}{2} S_{abcd}(\overline{\Phi}) \widetilde{K}_{cd}(\overline{\Phi}), \quad (52)$$

where the propagators \widetilde{K}_{ab} in the meson loops are given by (41). Inverting Eq. (52) leads to the following equation for the one meson-loop meson propagator

$$L_{ab} = K_{ab}(\overline{\Phi}) + \frac{1}{2} K_{ac}(\overline{\Phi}) S_{cdf}(\overline{\Phi}) \widetilde{K}_{de}(\overline{\Phi}) \widetilde{K}_{fg}(\overline{\Phi}) S_{egh}(\overline{\Phi}) L_{hb} - \frac{1}{2} K_{ac}(\overline{\Phi}) S_{cdef}(\overline{\Phi}) \widetilde{K}_{de}(\overline{\Phi}) L_{fb}. \quad (53)$$

The diagrammatic representation of this equation is presented in Fig. 3.

Despite the simple form (53) of the propagator $L(q^2)$, its numerical evaluation for arbitrary momentum is quite involved. It requires integration over the meson-loop four-momentum Q , over the momenta in the quark-loops as well as over the proper-time (or Feynman) parameters. Even after taking some of the integrals analytically we still end up with many-dimensional integrals, that must be evaluated numerically. However, we are first of all interested in pionic properties. Since the pion is very light we can determine the pion mass and the pion-quark coupling constant from the low-momentum expansion of the pion propagator. This leads to a radical simplification of the numerical calculation.

The inverse meson propagator in momentum space can be written in the form

$$L_{\alpha\beta}^{-1}(q^2) = L_{\alpha\beta}^{-1}(0) + \delta_{\alpha\beta} Z_{\alpha}(q^2) q^2. \quad (54)$$

The low-momentum expansion consists in calculating subsequent orders in q^2 . Expanding the inverse pion propagator up to second order gives

$$L_{\pi}^{-1}(q^2) = L_{\pi}^{-1}(0) + Z_{\pi}(0) q^2 + \mathcal{O}(q^4). \quad (55)$$

Both the constant term, $L_\pi^{-1}(0)$, and the q^2 -term, $Z_\pi(0)$, can be expressed as a sum of three contributions corresponding to the diagrams in Fig. 2. We present the straightforward but tedious evaluation of the diagrams in App. B.

We will now check that the pion remains massless when the $\frac{1}{N_c}$ meson-loop corrections are taken into account. The use of the one meson-loop gap equation is crucial for the proof. It is important that the gap equation is determined from the stationary-point condition for the effective action. We note that at the one meson-loop level the stationary point of the effective action and the quark self energy do not coincide. In the approaches of Refs. [9–11] where the gap equation at the one meson-loop level includes the quark self-energy diagram the Goldstone theorem does not hold. It does hold in the work of Ref. [12], where the quark self energy diagram has been replaced by a tadpole diagram. Thus contributions of the same order in N_c as the calculated meson-loop correction have been excluded in order to fulfill the Goldstone theorem. The retained tad-pole diagram is exactly the one obtained by dressing the quark propagator by a general static potential and hence in the approach of Ref. [12] one can recognize a symmetry conserving approximation [14].

In order to check the validity of the Goldstone theorem we have to evaluate the leading-order term $L_\pi^{-1}(0)$ in the low-momentum expansion of the inverse pion propagator. We write the inverse pion propagator at zero momentum as a sum of the contributions of the three diagrams in Fig. 2, in which we have now couplings with zero external pion momentum. This leads to a significant simplification in the evaluation of the diagrams. We present the calculation in App. B.2. Adding up all contributions we end with

$$L_\pi^{-1}(0) = (a^2 - 8N_c g(M)) + N_c \frac{1}{4\pi^2} \int_0^{\Lambda_b^2} d(Q^2) Q^2 \left\{ 4f(M, Q^2) \widetilde{K}_{00}(Q^2) + \sum_{\alpha\beta} \left(2f(M, 0) - f_1(M, Q^2)(Q^2 + 4M^2 \delta_{\alpha 0}) \right) \widetilde{K}_{\alpha\beta}(Q^2) \right\}. \quad (56)$$

Using in (56) the one meson-loop gap equation (45) we obtain

$$L_\pi^{-1}(0) = a^2 \frac{m}{M}, \quad (57)$$

which is analogous to the one quark-loop result with M_0 replaced by M . In the chiral limit ($m = 0$) we have $L_\pi^{-1}(0) = 0$, showing that the pions are massless. Thus, the Goldstone theorem is satisfied in the one meson-loop approximation.

This is a general feature. If we derive both the gap equation and the meson propagators by performing functional derivatives of the effective action, we have a symmetry-conserving approximation. The Goldstone pion reflects this.

For non-vanishing quark current mass m the chiral symmetry is explicitly broken and the pion acquires a finite mass. It is given by the position of the pole of the pion propagator. Using the inverse propagator in the form (54) we

obtain

$$L_\pi^{-1}(-m_\pi^2) = L_\pi^{-1}(0) - Z_\pi(-m_\pi^2) m_\pi^2 = 0 \quad (58)$$

and using Eq. (57) we obtain the on-shell pion mass as a solution of the following equation

$$m_\pi^2 = \frac{a^2 m}{Z_\pi(-m_\pi^2) M}. \quad (59)$$

Since m_π is very small we can approximate $Z_\pi(-m_\pi^2)$ by its value at zero momentum. Then we can calculate the pion mass in one meson-loop approximation using the results for the low-momentum expansion of the pion propagator

$$m_\pi^2 = \frac{a^2 m}{Z_\pi(0) M} + \mathcal{O}(m_\pi^4). \quad (60)$$

This equation has again exactly the same form as at the one quark-loop level.

The pion-quark coupling constant can be determined on the one meson-loop level similarly to (32) as the residue of the pion propagator (54) at its pole

$$g_{\pi qq}^2 = \lim_{q^2 \rightarrow -m_\pi^2} (q^2 + m_\pi^2) L_\pi^{-1}(q^2). \quad (61)$$

In the chiral limit we obtain the simple result

$$g_{\pi qq} = (Z_\pi(0))^{-\frac{1}{2}}. \quad (62)$$

7 Pion decay constant

In this section we present briefly the calculation of the pion decay constant F_π . It is an important quantity in our calculations, since we will later use its empirical value in order to fix the parameters of the model. This calculation allows us also to check explicitly the Goldberger-Treiman relation for the quarks giving the connection between the constituent quark mass, the pion-quark coupling constant and the pion decay constant. The Gell-Mann–Oakes–Renner relation follows then straightforwardly.

The pion decay constant F_π is defined by the matrix element for the weak pion decay

$$\langle 0 | A_\mu^a(z) | \pi^b(q) \rangle = -i \delta^{ab} q_\mu F_\pi e^{-iq \cdot z}, \quad (63)$$

where A_μ^a is the axial current and $\vec{\pi}$ is the physical pion field $\vec{\pi} = \vec{P}/g_{\pi qq}$. Applying the Lehmann-Symanzik-Zimmermann reduction formula we can relate the pion decay constant $F_\pi = F(-m_\pi^2)$ to the form factor $F(q^2)$, which can be expressed in terms of the expectation value of the time-ordered product

$$\langle 0|T[A_\mu^a(z), \pi^b(0)]|0\rangle = -i\delta^{ab} \int \frac{d^4q}{(2\pi)^4} F(q^2) \frac{q_\mu}{q^2 + m_\pi^2} e^{-iq \cdot z}. \quad (64)$$

To evaluate this matrix element we couple an external axial source j_μ^a in the effective action, which gives for the Dirac operator (*cf.* Eq. (8))

$$D = \beta \left(-i\not{\partial} + \Gamma_b \Phi_b + \gamma^\mu \gamma_5 \frac{\tau_a}{2} j_\mu^a \right). \quad (65)$$

Inserting this operator in the action we obtain the generating functional in the presence of the source j_μ^a for the external axial field. Then the matrix element (64) can be expressed as a variation of the generating functional

$$\langle 0|T[A_\mu^a(z), \pi^b(0)]|0\rangle = \frac{1}{g_{\pi qq}} \left. \frac{\delta^2 W(\chi, j)}{\delta j_\mu^a(z) \delta \chi^b(0)} \right|_{\chi, j=0}, \quad (66)$$

where $W(\chi, j)$ is the generating functional with sources for both the meson fields and the external axial field. Comparing Eqs. (64) and (66) we obtain

$$-i\delta_{ab} \int \frac{d^4q}{(2\pi)^4} F(q^2) \frac{q_\mu}{q^2 + m_\pi^2} e^{-iq \cdot z} = \frac{1}{g_{\pi qq}} \left. \frac{\delta^2 W(\chi, j)}{\delta j_\mu^a(z) \delta \chi^b(0)} \right|_{\chi, j=0}. \quad (67)$$

The rhs of this equation has the same structure as the one meson-loop pion propagator (11) with one derivative with respect to the meson source replaced by a derivative with respect to the axial source. Hence, in the one meson-loop approximation, we obtain contributions to the pion decay constant from diagrams analogous to those contributing to the inverse meson propagators (Fig. 2), but with one of the external meson couplings replaced by an axial coupling.

We calculate F_π from the low-momentum expansion as we did for the one meson-loop pion propagator. The difference is that now we pick up the terms linear in the external momentum q_μ (see Eq. 67). Also, due to the axial coupling, we obtain different spin-isospin structure of the quark-loop functions. Since the calculation is tedious and in the main steps analogous to the evaluation of the pion propagator we do not present details here. Calculating the pion decay constant in the chiral limit, $F_\pi = F(0)$, and using the expression for the pion-quark coupling constant (62) yields the Goldberger-Treiman relation [23] for the quarks

$$g_{\pi qq} F_\pi = M. \quad (68)$$

Using this result and the expressions for the pion mass (60) and the quark condensate (47) at the one meson-loop level we recover also the Gell-Mann–Oakes–Renner relation [24]

$$m\langle\bar{q}q\rangle = -m_\pi^2 F_\pi^2 + \mathcal{O}(m_\pi^4). \quad (69)$$

We have shown that in our effective action approach the Goldstone theorem, the Goldberger-Treiman, and the Gell-Mann–Oakes–Renner relations are valid with the meson loops included. Thus the basic relations following from Ward-Takahashi identities are satisfied in the one meson-loop approximation. Again, this is a feature of a symmetry-conserving approximation.

8 Results and discussion

At the one quark-loop level the model has the following parameters: the quark-quark coupling constant $G = \frac{1}{a^2}$, the fermionic cut-off Λ_f , and the current quark mass m . With the meson loop included we have, in addition, the bosonic cut-off Λ_b .

We use the empirical values for the observables in the meson sector, namely $F_\pi = 93$ MeV, and $m_\pi = 139$ MeV in order to fix the model parameters. After fitting the pion mass and decay constant, we are left with two free parameters. We could fix one of them by fitting the phenomenological value of the quark condensate $\langle\bar{q}q\rangle$. The results of our calculation for $\langle\bar{q}q\rangle$, however, are quite sensitive to the cut-off procedure. Furthermore, the experimental range for $\langle\bar{q}q\rangle$ is very wide ($(-\frac{1}{2}\langle\bar{q}q\rangle)_{\text{exp}}^{\frac{1}{3}} = 250 \pm 50$ MeV). For these reasons we do not use the value of the quark condensate to fix the parameters. Since we do not know the particular physics underlying the regularization of the theory, QCD cannot be a guide to fix the loop cut-offs Λ_f and Λ_b . In this exploratory calculation we display results obtained for four values of the ratio $\Lambda_b/\Lambda_f = 0, 0.5, 1$, and 1.5 . Using the gap equation we eliminate the coupling constant G in favor of the constituent quark mass M which we treat as a free parameter. Thus all quantities are presented as a function of M for different values of the ratio Λ_b/Λ_f .

We present the calculations performed in the chiral limit ($m = 0$). Introducing a nonzero current quark mass m leads to small corrections to the calculated quantities. Since at this point we are mainly interested in the general behavior of the constituent quark mass and the quark condensate as functions of the model parameters we find it useful to start by considering the chiral limit.

The constituent quark mass M in one meson-loop approximation is given by the solution of the gap equation (39). We use this equation in order to determine the fermionic cut-off Λ_f for given values of M and Λ_b/Λ_f . We plot Λ_f as a function of the constituent quark mass M for different values of the ratio Λ_b/Λ_f of the bosonic to the fermionic cut-off. The results in the chiral limit ($m = 0$) with proper-time and $O(4)$ fermion-loop regularization are presented in Figs. 4 and 5, respectively. The pion decay constant F_π is fitted to reproduce the experimental value. For $\Lambda_b = 0$ we recover the results of the one

fermion-loop approximation, so that the difference between the lowest curve and the other curves is a measure of the meson loop contribution. For Λ_f lower than a critical value we do not have spontaneous breaking of the chiral symmetry and the gap equation (25) has no solution. With increasing mesonic cut-off Λ_b the critical value of Λ_f increases and the curve “moves” up until Λ_b/Λ_f reaches ~ 1.5 for the proper-time cut-off and ~ 1.2 for the $O(4)$ one. For larger values of Λ_b/Λ_f the minimal value of Λ_f starts decreasing and the curve moves down with increasing Λ_b/Λ_f . This differs from the results of Dmi-trašinović *et al.* [12] with Pauli-Villars fermion-loop regularization where the curves keep moving towards larger values of Λ_f as Λ_b/Λ_f increases (see Fig. 11 in [12]). For large mesonic cut-offs, Λ_b/Λ_f over 2 for the proper-time fermion regularization and Λ_b/Λ_f over 3 in the $O(4)$ case, we do not have solution of the gap equation with F_π fitted to the experimental value. Calculations in the baryon sector of the Nambu–Jona-Lasinio model with one fermion and zero boson loops [25,26] show that best results for baryonic properties are obtained for M in the range 400–500 MeV, *i.e.* for values of the quark cut-off near the critical value. Although this picture may change when meson-loop effects are included, we note that the value of the constituent quark mass for the critical value of the quark cut-off changes very little. For $\Lambda_b \sim \Lambda_f$ the fermion cut-off increases by about 30%.

Comparing the results of the two fermion-loop regularization procedures we can see that although the critical values of Λ_f , below which there is no spontaneous chiral symmetry breaking are quite different, the general behavior of M as a function of the fermionic and mesonic cut-offs is very similar.

The quark condensate is given in terms of the constituent quark mass and the quark-quark coupling constant by Eq. (47). The results in the chiral limit are shown in Figs. 6 and 7 for the proper-time and $O(4)$ fermion-loop regularizations. They are plotted as a function of the constituent quark mass M for the four different ratios Λ_b/Λ_f . The empirical value for the quark condensate is obtained in chiral perturbation theory using the value of the quark current mass (Gell-Mann–Oakes–Renner relation) [27] or from QCD sum-rules. The phenomenological uncertainty (49) is, however, quite wide. With both the proper-time and $O(4)$ cut-offs there is a plateau for M between 0.3 and 0.6 GeV and the corresponding value of $\langle \bar{q}q \rangle$ depends little on Λ_b/Λ_f . The value in the proper-time case (Fig. 6) is underestimated. This problem is known from the one quark-loop calculations, where better agreement can be obtained using a generalized two-parameter proper-time regularization function. In the case of the $O(4)$ quark-loop regularization (Fig. 7) our results for the quark condensate are in the phenomenological bounds for values of M in the plateau region. This shows that the quark condensate is sensitive to the particular quark-loop regularization procedure, a feature well known from the calculations in the one quark-loop approximation.

In Fig. 8 we plot the ratio of the meson-loop to the quark-loop contribution to $\langle \bar{q}q \rangle$ as a function of M for the proper-time quark-loop regularization. The relative contribution of the meson loop increases with increasing Λ_b/Λ_f . For values of the parameters in the range $0.3 < M < 0.6$ GeV and $\Lambda_b/\Lambda_f < 1$ we have $\langle \bar{q}q \rangle_{\text{meson}}/\langle \bar{q}q \rangle_{\text{quark}} < 40\%$, *i.e.* of the order of $\frac{1}{N_c}$ as expected.

Looking at Figs. 6 and 8 we see that as Λ_b/Λ_f increases the meson-loop con-

tribution to the quark condensate increases, while the quark-loop contribution decreases. The sum of the contributions remains roughly constant. Eq. (47) shows that the inclusion of the meson-loops does not significantly change the four-quark coupling constant $G = \frac{1}{a^2}$.

Let us now come back to the N_c -counting scheme, which we extensively used throughout the meson-loop calculations presented above. We have calculated the meson-loop corrections to the constituent quark mass, the pion propagator and the pion decay constant, showing that they are one order in N_c suppressed. However, the expansion in powers of $\frac{1}{N_c}$ should be used with care since $N_c = 3$. Furthermore, the meson-loop corrections depend on the mesonic cut-off Λ_b and are infinite for $\Lambda_b \rightarrow \infty$. Hence it is important to check how well does the N_c -counting scheme work for the particular values of the parameters.

In the previous section we have compared the meson-loop and quark-loop contributions to $\langle \bar{q}q \rangle$ and found that for reasonable values of the parameters the ratio $\langle \bar{q}q \rangle_{\text{meson}} / \langle \bar{q}q \rangle_{\text{quark}}$ is in the expected range. Here we compare the meson- and quark-loop contributions to F_π . Since we have fixed the parameters in order to reproduce the experimental value of the pion decay constant the sum of both contributions gives $F_{\pi,\text{quark}} + F_{\pi,\text{meson}} = 93 \text{ MeV}$, but their relative contributions depend on the choice of parameters. The meson-loop contribution is negative. In Fig. 9 we show the ratio $|F_{\pi,\text{meson}}/F_{\pi,\text{quark}}|$ with proper-time quark-loop regularization. The relative contribution of the meson-loop grows with increasing constituent quark mass M . It is larger for larger values of Λ_b/Λ_f . As we mentioned in the previous section, the empirical value of F_π can be only reproduced for Λ_b/Λ_f less than about 2, which sets an upper bound for the meson-loop cut-off. For values of Λ_b in this range and $M < 0.6 \text{ GeV}$ the meson-loop correction does not exceed 40% of the N_c -leading quark-loop term. This is important because it keeps the $\frac{1}{N_c}$ corrections in the expected range. It justifies *a posteriori* the use of the N_c -counting scheme. The above observations are also true for the quark condensate (see Fig. 8) as well as for the $O(4)$ fermionic regularization. In the case when $\Lambda_b \simeq \Lambda_f$ and $0.3 < M < 0.6 \text{ MeV}$ we find that the meson-loop contributions are of the order of $\frac{1}{N_c} = \frac{1}{3}$ compared to the leading-order contributions.

9 Conclusion

We have shown that the effective action formalism in the Nambu–Jona-Lasinio model leads to a symmetry-conserving approximation, allowing us include consistently meson-loop effects while preserving the usual properties associated with spontaneous chiral symmetry breaking (the Goldstone theorem, the Gell-Mann–Oaks–Renner relation, *etc.*). Indeed, meson-loop effects will destroy these properties unless both the gap equation and meson propagators are treated consistently. This has already been noticed in Ref. [12], where Feynman diagrams were used. In our approach the conservation of the symmetry properties is a natural consequence of the consistent application of the $\frac{1}{N_c}$ expansion. We have found that though meson-loop contributions are $\frac{1}{N_c}$ -suppressed as compared to the leading-order quark-loop contributions they lead to substantial corrections. For the physically reasonable values of the pa-

rameters the effects of meson loops to the pion decay constant and the quark condensate are of the expected order of 30%.

Acknowledgment

The authors acknowledge the support of the Volkswagen Foundation (EN, CC), the Bulgarian National Science Foundation, contract Φ -406 (EN, CC), of the Polish State Committee of Scientific Research, grant 2 P03B 188 09 (WB), and of the Alexander von Humboldt Foundation (GR, WB), as well as partial support by COSY, BMBF and PROCOPE.

A Quark-loop meson vertices

In our meson-loop calculations we need the meson vertices which couple different number of mesons (we need up to four) through a quark loop. They are given by the variations of the effective action with respect to the meson fields. To obtain these we first expand the action in powers of the meson field fluctuations around the stationary point. We perform the expansion for the proper-time regularized effective action. Using the proper-time expressions we can easily obtain the four-momentum regularized expressions as well.

We start from the proper-time regularized effective action

$$I = \frac{N_c}{2} \text{Tr} \int_{\Lambda_f^{-2}}^{\infty} \frac{ds}{s} e^{-sD^\dagger D} + \frac{a^2}{2} \Phi^2 - a^2 m \Phi_0, \quad (\text{A.1})$$

where $D^\dagger D$ is given by

$$D^\dagger D = \partial^\mu \partial_\mu + i(\not{\partial} \Gamma_a \Phi_a) + \Phi^2. \quad (\text{A.2})$$

The fields Φ are now fluctuating around the stationary-point constant fields which are of the form $\Phi^{\text{st}} = \{S, 0, 0, 0\}$

$$\Phi = \Phi^{\text{st}} + \delta\Phi. \quad (\text{A.3})$$

Expanding $D^\dagger D$ in terms of the meson field fluctuations we obtain

$$D^\dagger D \equiv G_0^{-1} + V, \quad (\text{A.4})$$

where

$$G_0^{-1} = \partial^\mu \partial_\mu + \Phi^{\text{st}2} \quad (\text{A.5})$$

is the zero-order term in $\delta\Phi$ which is diagonal in momentum space and the fluctuation term is given by

$$\begin{aligned} V &= V^{(1)} + V^{(2)}, \\ V^{(1)} &= 2\Phi_a^{\text{st}} \delta\Phi_a + i\Gamma_a (\not{\partial} \delta\Phi_a), \\ V^{(2)} &= (\delta\Phi)^2 \end{aligned} \quad (\text{A.6})$$

and consists of terms of first, $V^{(1)}$, and second order, $V^{(2)}$, in the field fluctuations. Next we expand the exponent in the fermionic part of the effective action (A.1) in powers of V using the Feynman-Schwinger-Dyson formula and the cyclic property of the trace

$$\begin{aligned}
I_f &= \frac{N_c}{2} \text{Tr} \int_{\Lambda_f^{-2}}^{\infty} \frac{ds}{s} \left(e^{-sD^\dagger D} \right) \\
&= \frac{N_c}{2} \text{Tr} \int_{\Lambda_f^{-2}}^{\infty} \frac{ds}{s} \left\{ e^{-sG_0^{-1}} - sV e^{-sG_0^{-1}} + \frac{s^2}{2} \int_0^1 du V e^{-s(1-u)G_0^{-1}} V e^{-suG_0^{-1}} \right. \\
&\quad - \frac{s^3}{3} \int_0^1 du \int_0^{1-u} dv V e^{-s(1-u-v)G_0^{-1}} V e^{-suG_0^{-1}} V e^{-svG_0^{-1}} \\
&\quad \left. + \frac{s^4}{4} \int_0^1 du \int_0^{1-u} dv \int_0^{1-u-v} dw V e^{-s(1-u-v-w)G_0^{-1}} V e^{-suG_0^{-1}} V e^{-svG_0^{-1}} V e^{-swG_0^{-1}} \right\} \quad (A.7)
\end{aligned}$$

The first term in this expansion (zero order in V) gives the quark contribution to the one quark-loop effective action (23). The term linear in $\delta\Phi$ cancels with the mesonic terms in the expansion of the action since we expand around the stationary point.

The term quadratic in $\delta\Phi$ acquires contributions from the linear and quadratic in V terms as well as from the mesonic part of the effective action. Evaluating it in momentum space and taking the second variation with respect to the meson fields we obtain

$$\begin{aligned}
S_{ab} &\equiv \frac{\delta^2 I}{\delta\Phi_\alpha(q_1)\delta\Phi_\beta(q_2)} \\
&= \delta_{\alpha\beta} \delta(q_1 + q_2) \left\{ 4N_c \left[f(S, q_1)(q_1^2 + 4S^2\delta_{\alpha 0}) - 2g(S) \right] + a^2 \right\}, \quad (A.8)
\end{aligned}$$

where the functions f and g are calculated in App. C. The vertex function (A.8) corresponds to the quark loop with two meson couplings depicted in Fig. 10.

The third order term in the expansion of the action I in powers of the field fluctuations $\delta\Phi$ acquires contributions from the second and third order in V terms in (A.7)

$$I^{(3)} = I^{(3A)} + I^{(3B)}, \quad (A.9)$$

$$I^{(3A)} = N_c \sum_{C_V}^2 \text{Tr} \int_{\Lambda_f^{-2}}^{\infty} ds \frac{s}{4} \int_0^1 du V^{(1)} e^{-s(1-u)G_0^{-1}} V^{(2)} e^{-suG_0^{-1}}, \quad (A.10)$$

$$\begin{aligned}
I^{(3B)} &= -N_c \text{Tr} \int_{\Lambda_f^{-2}}^{\infty} ds \frac{s^2}{6} \int_0^1 du \int_0^{1-u} dv V^{(1)} e^{-s(1-u-v)G_0^{-1}} \\
&\quad \times V^{(1)} e^{-suG_0^{-1}} V^{(1)} e^{-svG_0^{-1}}, \quad (A.11)
\end{aligned}$$

where \sum_{C_V} denotes the sum over the combinations of $V^{(1)}$ and $V^{(2)}$. Varying this expressions with respect to the meson fields we obtain the corresponding three-leg quark-meson vertex functions in momentum space

$$S_{abc}^{(A)} \equiv \frac{\delta^3 I^{(3A)}}{\delta \Phi_\alpha(q_1) \delta \Phi_\beta(q_2) \delta \Phi_\gamma(q_3)} = 8N_c \sum_P^{3!} \delta(q_1 + q_2 + q_3) \Phi_\alpha^{\text{st}} \delta_{\beta\gamma} \\ \times \int_{\Lambda_f^{-2}}^{\infty} ds s \int_0^1 du \int \frac{d^4 k}{(2\pi)^4} e^{-s(1-u)((k+q_1)^2+S^2)} e^{-su(k^2+S^2)}, \quad (\text{A.12})$$

$$S_{abc}^{(B)} \equiv \frac{\delta^3 I^{(3B)}}{\delta \Phi_\alpha(q_1) \delta \Phi_\beta(q_2) \delta \Phi_\gamma(q_3)} = -\frac{8N_c}{3} \sum_P^{3!} \delta(q_1 + q_2 + q_3) \\ \times \left(4\Phi_\alpha^{\text{st}} \Phi_\beta^{\text{st}} \Phi_\gamma^{\text{st}} + \delta_{\alpha\beta} \Phi_\gamma^{\text{st}} q_1 \cdot q_2 + \delta_{\beta\gamma} \Phi_\alpha^{\text{st}} q_2 \cdot q_3 + \delta_{\alpha\gamma} \Phi_\beta^{\text{st}} q_1 \cdot q_3 \right) \\ \times \int_{\Lambda_f^{-2}}^{\infty} ds s^2 \int_0^1 du \int_0^{1-u} dv \int \frac{d^4 k}{(2\pi)^4} \\ \times e^{-s(1-u-v)((k+q_1)^2+S^2)} e^{-su((k+q_1+q_2)^2+S^2)} e^{-sv(k^2+S^2)}, \quad (\text{A.13})$$

where we have introduced the notation \sum_P for the sum over the permutations of the couples of meson-field indices and momenta $\{(\alpha, q_1), (\beta, q_2), (\gamma, q_3), \dots\}$. Summing the two contributions we obtain finally

$$S_{abc} = S_{abc}^{(A)} + S_{abc}^{(B)} \quad (\text{A.14})$$

which is expressed by the diagrams in Fig. 11.

The fourth order term in the expansion of I in powers of the field fluctuations $\delta\Phi$ acquires contributions from the second, third and fourth order in V terms in (A.7)

$$I^{(4)} = I^{(4A)} + I^{(4B)} + I^{(4C)}, \quad (\text{A.15})$$

$$I^{(4A)} = N_c \text{Tr} \int_{\Lambda_f^{-2}}^{\infty} ds \frac{s}{4} \int_0^1 du V^{(2)} e^{-s(1-u)G_0^{-1}} V^{(2)} e^{-suG_0^{-1}}, \quad (\text{A.16})$$

$$I^{(4B)} = -N_c \sum_{C_V}^3 \text{Tr} \int_{\Lambda_f^{-2}}^{\infty} ds \frac{s^2}{6} \int_0^1 du \int_0^{1-u} dv \\ \times V^{(2)} e^{-s(1-u-v)G_0^{-1}} V^{(1)} e^{-suG_0^{-1}} V^{(1)} e^{-svG_0^{-1}}, \quad (\text{A.17})$$

$$I^{(4C)} = N_c \text{Tr} \int_{\Lambda_f^{-2}}^{\infty} ds \frac{s^3}{8} \int_0^1 du \int_0^{1-u} dv \int_0^{1-u-v} dw \\ \times V^{(1)} e^{-s(1-u-v-w)G_0^{-1}} V^{(1)} e^{-suG_0^{-1}} V^{(1)} e^{-svG_0^{-1}} V^{(1)} e^{-swG_0^{-1}}. \quad (\text{A.18})$$

We evaluate the traces in momentum space and vary with respect to the meson fields in order to obtain the corresponding contributions to the four-leg quark-meson vertex

$$S_{abcd}^{(A)} \equiv \frac{\delta^4 I^{(4A)}}{\delta\Phi_\alpha(q_1)\delta\Phi_\beta(q_2)\delta\Phi_\gamma(q_3)\delta\Phi_\delta(q_4)} = 2N_c \sum_P^{4!} \delta(q_1 + q_2 + q_3 + q_4) \\ \times \delta_{\alpha\beta}\delta_{\gamma\delta} \int_{\Lambda_f^{-2}}^{\infty} ds s \int_0^1 du \int \frac{d^4 k}{(2\pi)^4} e^{-s(1-u)((k+q_1+q_2)^2+S^2)} e^{-su(k^2+S^2)}, \quad (\text{A.19})$$

$$S_{abcd}^{(B)} \equiv \frac{\delta^4 I^{(4B)}}{\delta\Phi_\alpha(q_1)\delta\Phi_\beta(q_2)\delta\Phi_\gamma(q_3)\delta\Phi_\delta(q_4)} = -4N_c \sum_P^{4!} \delta(q_1 + q_2 + q_3 + q_4) \\ \times \delta_{\alpha\beta}\delta_{\gamma\delta} (q_3 \cdot q_4 + 4S^2\delta_{\gamma 0}) \int_{\Lambda_f^{-2}}^{\infty} ds s^2 \int_0^1 du \int_0^{1-u} dv \int \frac{d^4 k}{(2\pi)^4} \\ \times e^{-s(1-u-v)((k+q_1+q_2)^2+S^2)} e^{-su((k+q_1+q_2+q_3)^2+S^2)} e^{-sv(k^2+S^2)}, \quad (\text{A.20})$$

$$S_{abcd}^{(C)} \equiv \frac{\delta^4 I_{\text{eff}}^{(4C)}}{\delta\Phi_\alpha(q_1)\delta\Phi_\beta(q_2)\delta\Phi_\gamma(q_3)\delta\Phi_\delta(q_4)} = N_c \sum_P^{4!} \delta(q_1 + q_2 + q_3 + q_4) \\ \times \left[16\Phi_\alpha^{\text{st}}\Phi_\beta^{\text{st}}\Phi_\gamma^{\text{st}}\Phi_\delta^{\text{st}} + 4 \sum_{C_{V'}}^6 (\delta_{\mu\nu}\Phi_\kappa^{\text{st}}\Phi_\chi^{\text{st}} q_i \cdot q_j) + (\delta^{\alpha\beta}\delta^{\gamma\delta} - \delta^{\alpha\gamma}\delta^{\beta\delta} + \delta^{\alpha\delta}\delta^{\beta\gamma}) \right. \\ \left. \times ((q_1 \cdot q_2)(q_3 \cdot q_4) - (q_1 \cdot q_3)(q_2 \cdot q_4) + (q_1 \cdot q_4)(q_2 \cdot q_3)) \right] \\ \times \int_{\Lambda_f^{-2}}^{\infty} ds s^3 \int_0^1 du \int_0^{1-u} dv \int_0^{1-u-v} dw \int \frac{d^4 k}{(2\pi)^4} e^{-s(1-u-v-w)((k+q_1)^2+S^2)} \\ \times e^{-su((k+q_1+q_2)^2+S^2)} e^{-sv((k+q_1+q_2+q_3)^2+S^2)} e^{-sw(k^2+S^2)}, \quad (\text{A.21})$$

where in the last contribution $\sum_{C_{V'}}^6$ stays for the sum over combinations, originating from different orderings of the two terms in $V^{(1)}$ (A.6)

$$\begin{aligned} \sum_{C_{V'}}^6 (\delta_{\mu\nu} \Phi_\kappa^{\text{st}} \Phi_\chi^{\text{st}} q_i \cdot q_j) &\equiv \delta_{\alpha\beta} \Phi_\gamma^{\text{st}} \Phi_\delta^{\text{st}} q_1 \cdot q_2 + \delta_{\alpha\gamma} \Phi_\beta^{\text{st}} \Phi_\delta^{\text{st}} q_1 \cdot q_3 \\ &+ \delta_{\alpha\delta} \Phi_\beta^{\text{st}} \Phi_\gamma^{\text{st}} q_1 \cdot q_4 + \delta_{\beta\gamma} \Phi_\alpha^{\text{st}} \Phi_\delta^{\text{st}} q_2 \cdot q_3 + \delta_{\beta\delta} \Phi_\alpha^{\text{st}} \Phi_\gamma^{\text{st}} q_2 \cdot q_4 + \delta_{\gamma\delta} \Phi_\alpha^{\text{st}} \Phi_\beta^{\text{st}} q_3 \cdot q_4. \end{aligned} \quad (\text{A.22})$$

Summing up all contributions we obtain finally

$$S_{abcd} = S_{abcd}^{(A)} + S_{abcd}^{(B)} + S_{abcd}^{(C)} \quad (\text{A.23})$$

which is expressed by the diagrams in Fig. 12.

B Low-momentum expansion

B.1 One meson-loop gap equation

Here we evaluate the one meson-loop contributions to the gap equation. Using the decomposition of the three-leg quark-loop function (Fig. 11) we obtain the meson-loop diagram (Fig. 1 (b)) as a sum of three contributions which we show in Fig. 13. The diagrams (a), (b) and (c) in Fig. 13 carry symmetry factors $\frac{1}{3}$, $\frac{2}{3}$, and 1 respectively, which account for the number of equivalent diagrams with the particular coupling of the meson propagator to the single or double legs of the quark-loop vertex in Fig. 11 (a). Using the quark-loop function S_{abc}^A (A.12) with $\alpha = 0$, $q_1 = 0$, $q_2 = -q_3 = Q$ we obtain for the quark-loop functions in the diagrams in Fig. 13 (a), (b)

$$S_{0\beta\gamma}^{GA} = \delta_{\beta\gamma} 48 N_c S f(S, 0), \quad (\text{B.1})$$

$$S_{0\beta\gamma}^{GB}(Q^2) = \delta_{\beta 0} \delta_{\gamma 0} 48 N_c S f(S, Q^2). \quad (\text{B.2})$$

Setting $\alpha = 0$, $q_1 = 0$, $q_2 = -q_3 = Q$ in S_{abc}^B (A.13) we obtain the quark-loop functions in the diagram Fig. 13(c)

$$S_{0\beta\gamma}^{GC}(Q^2) = -\delta_{\beta\gamma} 8 N_c S (Q^2 + 4 S^2 \delta_{\beta 0}) f_1(S, Q^2). \quad (\text{B.3})$$

Summing up all terms we obtain the meson-loop contribution to the gap equation (39)

$$\begin{aligned} \frac{1}{2} S_{0bc}(\bar{\Phi}) \widetilde{K}_{bc}(\bar{\Phi}) &= \frac{1}{2} \int_{|Q| < \Lambda_b} \frac{d^4 Q}{(2\pi)^4} \\ &\times \sum_{\beta\gamma} \left(\frac{1}{3} S_{0\beta\gamma}^{GA}(Q^2) + \frac{2}{3} S_{0\beta\gamma}^{GB}(Q^2) + S_{0\beta\gamma}^{GC}(Q^2) \right) \widetilde{K}_{\beta\gamma}(S, Q^2) \end{aligned}$$

$$\begin{aligned}
&= \frac{N_c}{4\pi^2} \int_0^{\Lambda_b^2} d(Q^2) Q^2 \left\{ 4f(S, Q^2) \widetilde{K}_{00}(S, Q^2) \right. \\
&\quad \left. + \sum_{\beta\gamma} \left(2f(S, 0) - f_1(S, Q^2)(Q^2 + 4S^2\delta_{\beta 0}) \right) \widetilde{K}_{\beta\gamma}(S, Q^2) \right\}. \quad (B.4)
\end{aligned}$$

After adding the quark-loop contribution we obtain the one meson-loop gap equation in the form (45).

B.2 Pion propagator

The inverse pion propagator in one meson-loop approximation is given by Eq. (52)

$$\begin{aligned}
L_{rs}^{-1} &= K_{rs}^{-1}(\overline{\Phi}) - \frac{1}{2} S_{rce}(\overline{\Phi}) \widetilde{K}_{cd}(\overline{\Phi}) \widetilde{K}_{ef}(\overline{\Phi}) S_{dfs}(\overline{\Phi}) \\
&\quad + \frac{1}{2} S_{rs cd}(\overline{\Phi}) \widetilde{K}_{cd}(\overline{\Phi}) = A_{rs} + B_{rs} + C_{rs}, \quad (B.5)
\end{aligned}$$

where we have denoted the contributions of the three diagrams in Fig. 2 by A , B and C , respectively. We define the indices $r \equiv \{\rho, x_r\}$, $s \equiv \{\sigma, x_s\}$ to be running only over pion fields, whereas $a \equiv \{\alpha, x_a\}$, $b \equiv \{\beta, x_b\}, \dots$ are running, as before, over both pion and sigma fields

$$\rho, \sigma \in \{1, 2, 3\}; \quad \alpha, \beta, \gamma, \dots \in \{0, 1, 2, 3\}. \quad (B.6)$$

The quark-loop contribution (Fig. 2(a)), which is leading order in N_c gives

$$A_{rs} = K_{rs}^{-1}(\overline{\Phi}). \quad (B.7)$$

Next we evaluate the diagram (b) for the inverse pion propagator (Fig. 2). Using the decomposition (Fig. 11) of the three-leg quark-loop vertices we obtain three contributions to this diagram, which we show in Fig. 14. In this figure we show also the possible routings of the external momentum q between the internal pion and sigma lines which are determined by the parameter α . In the limit of large mesonic cut-off $\Lambda_b \rightarrow \infty$ the final result does not depend on the particular momentum routing. In the presence of the cut-off we average over the routings of the external momentum, *i.e.* we integrate over α from zero to one. This procedure is arbitrary, and other prescription could also be used. Denoting the contributions of the diagrams in Fig. 14 by B_A , B_B , and B_C , respectively we obtain

$$B_{rs} = -\frac{1}{2} S_{rce}(\overline{\Phi}) \widetilde{K}_{cd}(\overline{\Phi}) \widetilde{K}_{ef}(\overline{\Phi}) S_{dfs}(\overline{\Phi}) = B_{Ars} + B_{Brs} + B_{Crs}, \quad (B.8)$$

where

$$B_{Ars} = -\frac{1}{9} S_{rbc}^{B_A} \widetilde{K}_{bd} \widetilde{K}_{ce} S_{sde}^{B_A}, \quad (\text{B.9})$$

$$B_{Brs} = -S_{rbc}^{B_B} \widetilde{K}_{bd} \widetilde{K}_{ce} S_{sde}^{B_B}, \quad (\text{B.10})$$

$$B_{Crs} = -\frac{2}{3} S_{rbc}^{B_A} \widetilde{K}_{bd} \widetilde{K}_{ce} S_{sde}^{B_B}, \quad (\text{B.11})$$

where we have multiplied by the corresponding symmetry factors for connecting the two quark-loop meson vertices with meson propagators. The diagrams in Fig. 14 contain two types of meson vertices (Fig. 11 (a), (b)). We calculate them in the low-momentum expansion for the particular values of the four-momenta. Using Eq. (A.12) we obtain for the quark-loop vertex (a) in Fig. 11

$$S_{rbc}^{B_A} = \delta_{\rho\beta} \delta_{\gamma 0} 48 N_c M f \left(M, (Q - \alpha q)^2 \right), \quad (\text{B.12})$$

where we have used the definition (C.3) of the regularization function f . Expanding this quark-loop function in powers of the external momentum q we obtain

$$\begin{aligned} S_{rbc}^{B_A} = & \delta_{\rho\beta} \delta_{\gamma 0} 48 N_c M \left(f(M, Q^2) + (Q \cdot q) 2\alpha f'(M, Q^2) + q^2 \alpha^2 f'(M, Q^2) \right. \\ & \left. + (Q \cdot q)^2 2\alpha^2 f''(M, Q^2) \right) + \mathcal{O}(q^3), \end{aligned} \quad (\text{B.13})$$

where we used the derivatives f' and f'' with respect to the four-momentum squared defined in App. C. The low-momentum expansion of the quark-loop vertex (b) in Fig. 11 is obtained by the use of Eq. (A.13)

$$\begin{aligned} S_{rbc}^{B_B} = & \delta_{\rho\beta} \delta_{\gamma 0} 16 N_c M q \cdot (Q + (1 - \alpha)q) \int \frac{d^4 k}{(2\pi)^4} \int_{\Lambda_f^{-2}}^{\infty} ds s^2 \int_0^1 du \int_0^{1-u} dv \\ & \times e^{-s(1-u-v)((k+(1-\alpha)q)^2+M^2)} e^{-su((k-\alpha q)^2+M^2)} e^{-sv((k-Q)^2+M^2)} \\ = & \delta_{\rho\beta} \delta_{\gamma 0} 8 N_c M \left((Q \cdot q - (1 - \alpha)q^2) f_1(M, Q^2) \right. \\ & \left. + 4(Q \cdot q)^2 (1 - 2\alpha) f_2(M, Q^2) \right) + \mathcal{O}(q^3), \end{aligned} \quad (\text{B.14})$$

with the regularization functions f_1 and f_2 defined in App. C.

Next we evaluate the diagram (c) for the inverse pion propagator (Fig. 2). We use the decomposition (Fig. 12) of the four-leg quark-loop vertices to obtain the seven different contributions to this diagram, which we show in Fig. 15. Since these diagrams contain only one meson propagator the meson-loop momentum Q does not depend on the external momentum q and the low-momentum expansion in powers of q is obtained by expanding only the

quark-loop function. Summing up the contributions of all diagrams in Fig. 15 with the corresponding symmetry factors for connecting the legs of the quark-loop vertex with the meson propagator we obtain the full contribution of the diagram (c) in Fig. 2 in the form

$$\begin{aligned}
C_{rs} &= \frac{1}{2} \left(\frac{1}{3} S_{rs cd}^{C_A} + \frac{2}{3} S_{rs cd}^{C_B} + \frac{1}{6} S_{rs cd}^{C_C} + \frac{1}{6} S_{rs cd}^{C_D} \right. \\
&\quad \left. + \frac{2}{3} S_{rs cd}^{C_E} + \frac{2}{3} S_{rs cd}^{C_F} + \frac{1}{3} S_{rs cd}^{C_G} \right) \widetilde{K}_{cd} \\
&= C_{Ars} + C_{Brs} + C_{Crs} + C_{Drs} + C_{Ers} + C_{Frs} + C_{Grs}.
\end{aligned} \tag{B.15}$$

We calculate the quark-loop vertices in the low-momentum expansion for the particular values of the four-momenta. Using Eq. (A.19) we obtain the quark-loop functions for the diagrams (a) and (b) in Fig. 15

$$S_{rs cd}^{C_A} = \delta_{\rho\sigma} \delta_{\gamma\delta} 48 N_c f(M, 0). \tag{B.16}$$

This function is independent of q and contributes only to the leading order in the low-momentum expansion. For the quark-loop function $S_{rs cd}^{C_B}$ we get

$$\begin{aligned}
S_{rs cd}^{C_B} &= \delta_{\rho\gamma} \delta_{\sigma\delta} 48 N_c f(M, (q - Q)^2) \\
&= \delta_{\rho\gamma} \delta_{\sigma\delta} 48 N_c M \left(f(M, Q^2) + 2(Q \cdot q) f'(M, Q^2) + q^2 f'(M, Q^2) \right. \\
&\quad \left. + (Q \cdot q)^2 2f''(M, Q^2) \right) + \mathcal{O}(q^3),
\end{aligned} \tag{B.17}$$

Inserting the particular four-momenta in Eq. (A.20) we obtain the quark-loop functions for the diagrams (c), (d) and (e) in Fig. 15

$$S_{rs cd}^{C_C} = -\delta_{\rho\sigma} \delta_{\gamma\delta} 48 N_c (Q^2 + 4M^2 \delta_{\gamma 0}) f_1(M, Q^2). \tag{B.18}$$

This function is independent of q and contributes only to the leading order in the low-momentum expansion. For the quark-loop function $S_{rs cd}^{C_D}$ we get

$$\begin{aligned}
S_{rs cd}^{C_D} &= -\delta_{\rho\sigma} \delta_{\gamma\delta} 48 N_c q^2 f_1(M, q^2) \\
&= -\delta_{\rho\sigma} \delta_{\gamma\delta} 48 N_c q^2 f_1(M, 0) + \mathcal{O}(q^4).
\end{aligned} \tag{B.19}$$

For the quark-loop function $S_{rs cd}^{C_E}$ we obtain

$$\begin{aligned}
S_{rs cd}^{C_E} &= -\delta_{\rho\gamma} \delta_{\sigma\delta} 96 N_c (-Q \cdot q) \int \frac{d^4 k}{(2\pi)^4} \int_{\Lambda_f^{-2}}^{\infty} ds s^2 \int_0^1 du \int_0^{1-u} dv \\
&\quad \times e^{-s(1-u-v)(k^2+M^2)} e^{-su((k-q)^2+M^2)} e^{-sv((k-Q)^2+M^2)}
\end{aligned} \tag{B.20}$$

$$= -\delta_{\rho\gamma}\delta_{\sigma\delta} 48 N_c \left(-(Q \cdot q) f_1(M, Q^2) + 4(Q \cdot q)^2 f_2(M, Q^2) \right) + \mathcal{O}(q^3),$$

where the regularization function f_2 is calculated in App. C. There are two possibilities for coupling the meson-loop propagator to the four-leg quark-loop vertex (c) in Fig. 12—to adjacent (Fig. 15(f)) or to opposed (Fig. 15(g)) legs. Inserting the values of the four-momenta in Eq. (A.21) we calculate the quark-loop functions for adjacent meson-loop couplings

$$\begin{aligned} S_{rscd}^{CF} &= \delta_{\rho\sigma}\delta_{\gamma\delta} 24 N_c q^2 (Q^2 + 4M^2\delta_{\gamma 0}) \int \frac{d^4 k}{(2\pi)^4} \int_{\Lambda_f^{-2}}^{\infty} ds s^3 \int_0^1 du \int_0^{1-u} dv \int_0^{1-u-v} dw \\ &\quad \times e^{-s(1-u-v-w)(k^2+M^2)} e^{-su((k-Q)^2+M^2)} e^{-sv(k^2+M^2)} e^{-sw((k-q)^2+M^2)} \\ &= \delta_{\rho\sigma}\delta_{\gamma\delta} 12 N_c q^2 (Q^2 + 4M^2\delta_{\gamma 0}) f_3(M, Q^2) + \mathcal{O}(q^3), \end{aligned} \quad (\text{B.21})$$

and for opposed meson-loop couplings

$$\begin{aligned} S_{rscd}^{CG} &= \delta_{\rho\sigma}\delta_{\gamma\delta} 24 N_c \left((2(Q \cdot q)^2 - Q^2 q^2) (2\delta_{\rho\gamma} - 1) + 4q^2 M^2 \delta_{\gamma 0} \right) \\ &\quad \times \int \frac{d^4 k}{(2\pi)^4} \int_{\Lambda_f^{-2}}^{\infty} ds s^3 \int_0^1 du \int_0^{1-u} dv \int_0^{1-u-v} dw e^{-s(1-u-v-w)(k^2+M^2)} \\ &\quad \times e^{-su((k-Q)^2+M^2)} e^{-sv((k-Q-q)^2+M^2)} e^{-sw((k-q)^2+M^2)} \\ &= \delta_{\rho\sigma}\delta_{\gamma\delta} 96 N_c \left((2(Q \cdot q)^2 - Q^2 q^2) (2\delta_{\rho\gamma} - 1) + 4q^2 M^2 \delta_{\gamma 0} \right) \\ &\quad \times f_2(M, Q^2) + \mathcal{O}(q^3), \end{aligned} \quad (\text{B.22})$$

where the regularization functions f_2 and f_3 are calculated in App. C.

The low-momentum expansion of the pion propagator up to second order gives (55)

$$L_{\pi}^{-1}(q^2) = L_{\pi}^{-1}(0) + Z_{\pi}(0)q^2 + \mathcal{O}(q^4). \quad (\text{B.23})$$

We expand the contributions of the diagrams in Fig. 2 to the inverse pion propagator in powers of the external momentum q

$$A(q^2) = A^{(0)} + A^{(2)}q^2 + \mathcal{O}(q^4) \quad (\text{B.24})$$

and similarly for $B(q^2)$ and $C(q^2)$. Then we can write the terms of the expansion (B.23) as sum of the contributions of the diagrams in Fig. 2

$$L_{\pi}^{-1}(0) = A^{(0)} + B^{(0)} + C^{(0)}, \quad (\text{B.25})$$

$$Z_{\pi}(0) = A^{(2)} + B^{(2)} + C^{(2)}. \quad (\text{B.26})$$

We start by evaluating the contributions to the leading term $K^{-1}(0)$ in the low-momentum expansion of the inverse pion propagator. The leading- N_c diagram gives

$$A_{\rho\sigma}^{(0)} = \delta_{\rho\sigma}(-8N_c g(M) + a^2). \quad (\text{B.27})$$

At zero momentum we get non-vanishing contribution only from one diagram (b) of all diagrams in Fig. 14. Inserting the results for the low-momentum expansion of the corresponding quark-loop function (B.13) in Eq. (B.10) we obtain the contribution

$$\begin{aligned} B_{\rho\sigma}^{(0)} &= -256 N_c^2 M^2 \int_{|Q| < \Lambda_b} \frac{d^4 Q}{(2\pi)^4} \left(f(M, Q^2)\right)^2 \widetilde{K}_{\rho\sigma}(Q^2) \widetilde{K}_{00}(Q^2) \\ &= \frac{N_c}{\pi^2} \int_0^{\Lambda_b^2} d(Q^2) Q^2 f(M, Q^2) \left(\delta_{\rho\sigma} \widetilde{K}_{00}(Q^2) - \widetilde{K}_{\rho\sigma}(Q^2)\right), \end{aligned} \quad (\text{B.28})$$

where we have used the algebraic identity for the product of a sigma and a pion propagator at equal momenta

$$\widetilde{K}_{\rho\sigma}(Q^2) \widetilde{K}_{00}(Q^2) = \frac{1}{16N_c M^2 f(M, Q^2)} \left(\widetilde{K}_{\rho\sigma}(Q^2) - \delta_{\rho\sigma} \widetilde{K}_{00}(Q^2)\right). \quad (\text{B.29})$$

We have three non-vanishing contributions to $C^{(0)}$ from the diagrams (a), (b) and (c) in Fig. 15. Inserting the results for the low-momentum expansion of the corresponding quark-loop vertices (B.16), (B.17), (B.18) in Eq. (B.15) we obtain

$$\begin{aligned} C_{\rho\sigma}^{(0)} &= \delta_{\rho\sigma} \frac{N_c}{2\pi^2} f(M, 0) \int_0^{\Lambda_b^2} d(Q^2) Q^2 \sum_{\gamma\delta} \widetilde{K}_{\gamma\delta}(Q^2) \\ &\quad + \frac{N_c}{\pi^2} \int_0^{\Lambda_b^2} d(Q^2) Q^2 f(M, Q^2) \widetilde{K}_{\rho\sigma}(Q^2) \\ &\quad - \delta_{\rho\sigma} \frac{N_c}{4\pi^2} \int_0^{\Lambda_b^2} d(Q^2) Q^2 f_1(M, Q^2) \sum_{\gamma\delta} (Q^2 + 4M^2 \delta_{\gamma 0}) \widetilde{K}_{\gamma\delta}(Q^2). \end{aligned} \quad (\text{B.30})$$

Summing up all contributions we end up with

$$L_{\rho\sigma}^{-1}(0) = \delta_{\rho\sigma}(a^2 - 8N_c g(M)) + \delta_{\rho\sigma} \frac{N_c}{4\pi^2} \int_0^{\Lambda_b^2} d(Q^2) Q^2 \left\{ 4f(M, Q^2) \widetilde{K}_{00}(Q^2) \right.$$

$$+ \sum_{\gamma\delta} \left(2f(M, 0) - f_1(M, Q^2)(Q^2 + 4M^2\delta_{\gamma 0}) \right) \widetilde{K}_{\gamma\delta}(Q^2) \Big\}. \quad (\text{B.31})$$

This result allows us to check the validity of the Goldstone theorem at the one meson-loop level, which is seen immediately when comparing with Eq. (B.4).

Now we turn to the next to leading order (B.26) in the low-momentum expansion of the pion propagator. The quark-loop contribution $A^{(2)}$ is given by

$$A_{\rho\sigma}^{(2)} = \delta_{\rho\sigma} 4N_c f(M, 0). \quad (\text{B.32})$$

The term $B^{(2)}$, corresponding to the diagram with two internal meson lines consists of three contributions (see Fig. 14), which we denote by $B_A^{(2)}$, $B_B^{(2)}$, and $B_C^{(2)}$, respectively. We use the low-momentum expansion of the quark-loop vertices (B.13), (B.14) and expand the propagators for the internal meson lines in Eqs. (B.9), (B.10) and (B.11). Picking up the terms of order q^2 we obtain

$$\begin{aligned} B^{(2)} &= B_A^{(2)} + B_B^{(2)} + B_C^{(2)}, \\ B_{A\rho\sigma}^{(2)} &= -\frac{8N_c^2}{3\pi^2} M^2 \int_0^{\Lambda_b^2} d(Q^2) Q^2 \Big\{ 2 \Big[2f(M, Q^2) f'(M, Q^2) \widetilde{K}_{\rho\sigma}(Q^2) \widetilde{K}_{00}(Q^2) \\ &\quad + \left(f(M, Q^2) \right)^2 \left(\widetilde{K}'_{\rho\sigma}(Q^2) \widetilde{K}_{00}(Q^2) + \widetilde{K}_{\rho\sigma}(Q^2) \widetilde{K}'_{00}(Q^2) \right) \Big] \\ &\quad + Q^2 \Big[2 \left(\left(f'(M, Q^2) \right)^2 + f(M, Q^2) f''(M, Q^2) \right) \widetilde{K}_{\rho\sigma}(Q^2) \widetilde{K}_{00}(Q^2) \\ &\quad + \left(f(M, Q^2) \right)^2 \left(\widetilde{K}''_{\rho\sigma}(Q^2) \widetilde{K}_{00}(Q^2) \right. \\ &\quad \left. + \widetilde{K}_{\rho\sigma}(Q^2) \widetilde{K}''_{00}(Q^2) - \widetilde{K}'_{\rho\sigma}(Q^2) \widetilde{K}'_{00}(Q^2) \right) \\ &\quad \left. + 2f(M, Q^2) f'(M, Q^2) \left(2\widetilde{K}_{\rho\sigma}(Q^2) \widetilde{K}'_{00}(Q^2) - \widetilde{K}'_{\rho\sigma}(Q^2) \widetilde{K}_{00}(Q^2) \right) \right] \Big\}, \\ B_{B\rho\sigma}^{(2)} &= -\frac{N_c^2}{\pi^2} M^2 \int_0^{\Lambda_b^2} d(Q^2) Q^4 \Big\{ \left(f_1(M, Q^2) \right)^2 \widetilde{K}_{\rho\sigma}(Q^2) \widetilde{K}_{00}(Q^2) \Big\}, \\ B_{C\rho\sigma}^{(2)} &= \frac{4N_c^2}{\pi^2} M^2 \int_0^{\Lambda_b^2} d(Q^2) Q^2 \Big\{ 2f(M, Q^2) f_1(M, Q^2) \widetilde{K}_{\rho\sigma}(Q^2) \widetilde{K}_{00}(Q^2) \\ &\quad - Q^2 \Big[f'(M, Q^2) f_1(M, Q^2) \widetilde{K}_{\rho\sigma}(Q^2) \widetilde{K}_{00}(Q^2) \\ &\quad + f(M, Q^2) f_1(M, Q^2) \left(-\widetilde{K}'_{\rho\sigma}(Q^2) \widetilde{K}_{00}(Q^2) + \widetilde{K}_{\rho\sigma}(Q^2) \widetilde{K}'_{00}(Q^2) \right) \Big] \Big\}. \end{aligned} \quad (\text{B.33})$$

The term $C^{(2)}$ comes from the diagram (c) in Fig. 2 with one internal meson line and acquires contributions from the diagrams (b), (d), (e), (f) and (g) in Fig. 15. Using the results for the low-momentum expansion of the corresponding quark-loop vertices we obtain

$$\begin{aligned}
C^{(2)} &= C_B^{(2)} + C_D^{(2)} + C_E^{(2)} + C_F^{(2)} + C_G^{(2)}, \\
C_{B\rho\sigma}^{(2)} &= \frac{N_c}{2\pi^2} \int_0^{\Lambda_b^2} d(Q^2) Q^2 \left(2f'(M, Q^2) + Q^2 f''(M, Q^2) \right) \widetilde{K}_{\rho\sigma}(Q^2), \\
C_{D\rho\sigma}^{(2)} &= -\delta_{\rho\sigma} \frac{N_c}{4\pi^2} f_1(M, 0) \int_0^{\Lambda_b^2} d(Q^2) Q^2 \sum_{\gamma\delta} \widetilde{K}_{\gamma\delta}(Q^2), \\
C_{E\rho\sigma}^{(2)} &= -\frac{N_c}{\pi^2} \int_0^{\Lambda_b^2} d(Q^2) Q^4 f_2(M, Q^2) \widetilde{K}_{\rho\sigma}(Q^2), \\
C_{F\rho\sigma}^{(2)} &= \delta_{\rho\sigma} \frac{N_c}{4\pi^2} \int_0^{\Lambda_b^2} d(Q^2) Q^2 \sum_{\gamma\delta} (Q^2 + 4M^2 \delta_{\gamma 0}) f_3(M, Q^2) \widetilde{K}_{\gamma\delta}(Q^2), \\
C_{G\rho\sigma}^{(2)} &= \delta_{\rho\sigma} \frac{N_c}{2\pi^2} \int_0^{\Lambda_b^2} d(Q^2) Q^2 \sum_{\gamma\delta} \left(Q^2 (1 - 2\delta_{\rho\gamma}) + 8M^2 \delta_{\gamma 0} \right) \\
&\quad \times f_2(M, Q^2) \widetilde{K}_{\gamma\delta}(Q^2). \tag{B.34}
\end{aligned}$$

All regularization functions and the leading-order meson propagators involved in these expressions are listed for both the proper-time and $O(4)$ cut-offs in App. C. Summing up all contributions from (B.32), (B.33) and (B.34) we obtain the second order term in the low-momentum expansion (B.23) of the pion propagator.

C Regularization functions

Here we calculate the regularization functions for the quark-loop vertices in the diagrams for the one meson-loop gap equation and pion propagator. We start by evaluating the regulators in the proper-time scheme. The $O(4)$ regulators can be then easily obtained using the intermediate results for the proper-time ones.

C.1 Proper-time regularization

We start by evaluating the function g emerging in the one fermion-loop gap equation. It is given by

$$\begin{aligned}
g(S) &\equiv \int \frac{d^4 k}{(2\pi)^4} \int_{\Lambda_f^{-2}}^{\infty} ds e^{-s(k^2+S^2)} \\
&= \frac{1}{16\pi^2} \left(\Lambda_f^2 e^{-\frac{S^2}{\Lambda_f^2}} - S^2 E_1 \left(\frac{S^2}{\Lambda_f^2} \right) \right),
\end{aligned} \tag{C.1}$$

where E_1 is the exponential integral defined by

$$E_n(x) \equiv \int_1^{\infty} dt \frac{e^{-xt}}{t^n}. \tag{C.2}$$

The function f is defined by

$$\begin{aligned}
f(S, q^2) &\equiv \int \frac{d^4 k}{(2\pi)^4} \int_{\Lambda_f^{-2}}^{\infty} ds s \int_0^1 du e^{-s(1-u)((k+\frac{q}{2})^2+S^2)} e^{-su((k-\frac{q}{2})^2+S^2)} \\
&= \frac{1}{16\pi^2} \int_0^1 du E_1 \left(\frac{S^2 + u(1-u)q^2}{\Lambda_f^2} \right).
\end{aligned} \tag{C.3}$$

The function f_1 , which appears in the one meson-loop gap equation reads

$$\begin{aligned}
f_1(S, q^2) &\equiv \int \frac{d^4 k}{(2\pi)^4} \int_{\Lambda_f^{-2}}^{\infty} ds s^2 \int_0^1 du e^{-s(1-u)((k+\frac{q}{2})^2+S^2)} e^{-su((k-\frac{q}{2})^2+S^2)} \\
&= \frac{1}{16\pi^2} \int_0^1 du \frac{1}{S^2 + u(1-u)q^2} e^{-\frac{S^2 + u(1-u)q^2}{\Lambda_f^2}}.
\end{aligned} \tag{C.4}$$

For the evaluation of the one meson-loop pion propagator we need the derivatives of the function $f(S, q^2)$ with respect to q^2

$$\begin{aligned}
f'(S, q^2) &\equiv \frac{\partial f(S, q^2)}{\partial(q^2)} \\
&= -\frac{1}{16\pi^2} \int_0^1 du u(1-u) \frac{1}{S^2 + u(1-u)q^2} e^{-\frac{S^2 + u(1-u)q^2}{\Lambda_f^2}},
\end{aligned} \tag{C.5}$$

$$f''(S, q^2) \equiv \frac{\partial^2 f(S, q^2)}{\partial(q^2)^2}$$

$$= \frac{1}{16\pi^2} \int_0^1 du u^2 (1-u)^2 \frac{S^2 + u(1-u)q^2 + \Lambda_f^2}{\Lambda_f^2 (S^2 + u(1-u)q^2)^2} e^{-\frac{S^2 + u(1-u)q^2}{\Lambda_f^2}}. \quad (\text{C.6})$$

In the derivation of the one meson-loop pion propagator we have used the leading-order meson propagators (41) and their derivatives with respect to q^2

$$\widetilde{K}_{\alpha\beta}(q^2) = \delta_{\alpha\beta} \left(4N_c f(S, q^2) (q^2 + 4S^2) \right)^{-1}, \quad (\text{C.7})$$

$$\begin{aligned} \widetilde{K}'_{\alpha\beta}(q^2) &\equiv \frac{\partial K_{\alpha\beta}(q^2)}{\partial(q^2)} \\ &= -4N_c \widetilde{K}_{\alpha\beta}^2(q^2) \left(f'(S, q^2) (q^2 + 4S^2 \delta_{\alpha 0}) + f(S, q^2) \right), \end{aligned} \quad (\text{C.8})$$

$$\begin{aligned} \widetilde{K}''_{\alpha\beta}(q^2) &\equiv \frac{\partial^2 K_{\alpha\beta}(q^2)}{\partial(q^2)^2} \\ &= 32N_c^2 \widetilde{K}_{\alpha\beta}^3(q^2) \left(f'(S, q^2) (q^2 + 4S^2 \delta_{\alpha 0}) + f(S, q^2) \right)^2 \\ &\quad - 4N_c \widetilde{K}_{\alpha\beta}^2(q^2) \left(f''(S, q^2) (q^2 + 4S^2 \delta_{\alpha 0}) + 2f'(S, q^2) \right). \end{aligned} \quad (\text{C.9})$$

For the low-momentum expansion of $S_{rscd}^{C_e}$ (B.20) we have to evaluate

$$\begin{aligned} &\frac{\partial}{\partial(Q \cdot q)} \left\{ \int \frac{d^4 k}{(2\pi)^4} \int_{\Lambda_f^{-2}}^{\infty} ds s^2 \int_0^1 du \int_0^{1-u} dv \right. \\ &\quad \left. \times e^{-s(1-u-v)(k^2+M^2)} e^{-su((k-q)^2+M^2)} e^{-sv((k-Q)^2+M^2)} \right\} \Big|_{q=0} \\ &= 2f_2(M, Q^2), \end{aligned} \quad (\text{C.10})$$

where we define the regularization function

$$\begin{aligned} f_2(S, q^2) &\equiv \frac{1}{16\pi^2} \int_{\Lambda_f^{-2}}^{\infty} ds s \int_0^1 du \int_0^{1-u} dv uv e^{-s(S^2+v(1-v)q^2)} \\ &= \frac{1}{64\pi^2} \int_0^1 du u(1-u) \frac{S^2 + u(1-u)q^2 + \Lambda_f^2}{\Lambda_f^2 (S^2 + u(1-u)q^2)^2} e^{-\frac{S^2 + u(1-u)q^2}{\Lambda_f^2}}. \end{aligned} \quad (\text{C.11})$$

Similarly, for the low-momentum expansion of $S_{rbc}^{B_b}$ (B.14) we have to evaluate

$$\frac{\partial}{\partial(Q \cdot q)} \left\{ \int \frac{d^4 k}{(2\pi)^4} \int_{\Lambda_f^{-2}}^{\infty} ds s^2 \int_0^1 du \int_0^{1-u} dv \right.$$

$$\begin{aligned}
& \times e^{-s(1-u-v)((k+(1-\alpha)q)^2+S^2)} e^{-su((k-\alpha q)^2+S^2)} e^{-sv((k-Q)^2+S^2)} \Bigg|_{q=0} \\
& = 2(1-2\alpha)f_2(S, Q^2). \tag{C.12}
\end{aligned}$$

In the low-momentum expansion of $S_{rscl}^{C_f}$ (B.21) we obtain the regularization function

$$\begin{aligned}
f_3(S, q^2) &= \frac{1}{16\pi^2} \int_{\Lambda_f^{-2}}^{\infty} ds s \int_0^1 du u^2 e^{-s(S^2+u(1-u)q^2)} \\
&= \frac{1}{16\pi^2} \int_0^1 du u^2 \frac{S^2 + u(1-u)q^2 + \Lambda_f^2}{\Lambda_f^2 (S^2 + u(1-u)q^2)^2} e^{-\frac{S^2+u(1-u)q^2}{\Lambda_f^2}}. \tag{C.13}
\end{aligned}$$

Finally, taking the k -integral in $S_{rscl}^{C_g}$ (B.22) we obtain

$$\begin{aligned}
& \frac{1}{16\pi^2} \int_{\Lambda_f^{-2}}^{\infty} ds s \int_0^1 du \int_0^{1-u} dv (1-u-v) e^{-s(S^2+(u+v)(1-u-v)q^2)} \\
& = 4 f_2(S, q^2). \tag{C.14}
\end{aligned}$$

C.2 $O(4)$ regularization

Here we define the quark-loop $O(4)$ regularization. The running four-momentum of the quark loop is limited in the following manner. We obtain the quark-loop vertex functions in our $O(4)$ regularization scheme using the intermediate results from the proper-time calculation. After having completed the square for the fermion-loop four-momentum k in the proper-time expressions we take the limit in the *proper-time* fermionic cut-off $\Lambda_f^{PT} \rightarrow \infty$ using the identity

$$\lim_{\Lambda_f^{PT} \rightarrow \infty} \int_{(\Lambda_f^{PT})^{-2}}^{\infty} ds s^n e^{-sA} = \frac{n!}{A^{n+1}}, \quad \text{for } n \geq 0, A > 0. \tag{C.15}$$

Then we cut off the integral at some $O(4)$ cut-off $\Lambda_f^{O(4)}$ and obtain the $O(4)$ regularization functions. Note that in the following expressions both the k^2 - and u -integrals can be taken analytically. This leads, however, to quite lengthy sums of logarithms and rational functions, and for the sake of clarity we present the regularization functions keeping the integrals.

The function $g(S)$ can be easily obtained from the $O(4)$ -regularized action

$$g(S) = \frac{1}{16\pi^2} \int_0^{\Lambda_f^2} d(k^2) \frac{k^2}{k^2 + S^2}, \quad (C.16)$$

Using Eqs. (C.3), (C.4) we obtain

$$f(S, q^2) = \frac{1}{16\pi^2} \int_0^{\Lambda_f^2} d(k^2) \int_0^1 du \frac{k^2}{(k^2 + S^2 + u(1-u)q^2)^2}, \quad (C.17)$$

$$f_1(S, q^2) = \frac{1}{8\pi^2} \int_0^{\Lambda_f^2} d(k^2) \int_0^1 du \frac{k^2}{(k^2 + S^2 + u(1-u)q^2)^3}. \quad (C.18)$$

The functions f' and f'' can be easily obtained taking the derivatives of Eq. (C.17)

$$f'(S, q^2) = -\frac{1}{8\pi^2} \int_0^{\Lambda_f^2} d(k^2) \int_0^1 du \frac{k^2 u(1-u)}{(k^2 + S^2 + u(1-u)q^2)^3}, \quad (C.19)$$

$$f''(S, q^2) = \frac{3}{8\pi^2} \int_0^{\Lambda_f^2} d(k^2) \int_0^1 du \frac{k^2 u^2(1-u)^2}{(k^2 + S^2 + u(1-u)q^2)^4}. \quad (C.20)$$

Using Eqs. (C.11), (C.13) we get

$$f_2(S, q^2) = \frac{3}{32\pi^2} \int_0^{\Lambda_f^2} d(k^2) \int_0^1 du \frac{k^2 u(1-u)}{(k^2 + S^2 + u(1-u)q^2)^4}, \quad (C.21)$$

$$f_3(S, q^2) = \frac{3}{8\pi^2} \int_0^{\Lambda_f^2} d(k^2) \int_0^1 du \frac{k^2 u^2}{(k^2 + S^2 + u(1-u)q^2)^4}. \quad (C.22)$$

References

- [1] Y. Nambu and G. Jona-Lasinio, Phys. Rev. 122 (1961) 345
- [2] W. Weise, Univ. of Regensburg preprint TPR-93-2
- [3] U. Vogl and W. Weise, Progr. Part. Nucl. Phys. 7 (1991) 195

- [4] J. Bijnens, Nordita preprint No. 95-10-N-P, hep-ph/9502335 (1995)
- [5] R. Alkofer, H. Reinhardt, and H. Weigel, Univ. Tübingen preprint No. UNITU-THEP-25/1994 (1994)
- [6] Chr. V. Christov *et al.*, Ruhr-Univ. Bochum preprint No. RUB-TPII-32-95 (1995)
- [7] S. Krewald, K. Nakayama, and J. Speth, Phys. Lett. B272 (1991) 190
- [8] L. S. Celenza, A. Pantziris, C. M. Shakin, and J. Szweda, Phys. Rev. C47 (1993) 2356
- [9] N.-W. Cao, C. M. Shakin, and W.-D. Sun, Phys. Rev. C46 (1992) 2535
- [10] P. P. Domitrovich, D. Bückers, and H. Müther, Phys. Rev. C48 (1993) 413
- [11] E. Quack and S. P. Klevansky, Phys. Rev. C49 (1994) 3283; P. Zhuang, J. Hüfner, and S. P. Klevansky, Nucl. Phys. A576 (1994) 525; P. Zhuang, J. Hüfner, S. P. Klevansky, and H. Voss, Ann. Phys. (N.Y.) 234 (1994) 225
- [12] V. Dmitrašinović, H.-J. Schulze, R. Tegen, and R. H. Lemmer, Ann. Phys. (N.Y.) 238 (1995) 332
- [13] L. P. Kadanoff and G. Baym, Quantum Statistical Mechanics (Benjamin, New York, 1962)
- [14] J.-P. Blaizot and G. Ripka, Quantum Theory of Finite Systems (MIT Press, Cambridge, 1986)
- [15] T. Eguchi, Phys. Rev. D 14 (1975) 2755
- [16] S. Coleman and E. Weinberg, Phys. Rev. D7 (1973) 1888
- [17] C. Itzykson and J.-B. Zuber, Quantum Field Theory (McGraw-Hill, New York, 1980)
- [18] R. Paden and G. Ripka, Nucl. Phys. A149 (1970) 273
- [19] M. Jaminon, R. M. Galain, G. Ripka, and P. Stassart, Nucl. Phys. A537 (1992) 418
- [20] G. 't Hooft, Nucl. Phys. B75 (1974) 461
- [21] E. Witten, Nucl. Phys. B160 (1979) 57
- [22] S. Narison, QCD Sum Rules (World Scientific, Singapore, 1990)
- [23] M. Goldberger and S. Treiman, Phys. Rev. 110 (1958) 1178

- [24] M. Gell-Mann, R. Oakes, and B. Renner, Phys. Rev. 175 (1968) 2195
- [25] Th. Meissner and K. Goeke, Nucl. Phys. A524 (1991) 719
- [26] Chr. V. Christov, A. Z. Górski, K. Goeke, and P. V. Pobylitsa, Nucl. Phys. A592 (1995) 513
- [27] J. Gasser and H. Leutwyler, Phys. Rep. 87 (1982) 77

$$\begin{array}{ccccccc}
 \times & + & \text{a} & + \frac{1}{2} & \text{b} & = & 0
 \end{array}$$

Fig. 1. The diagrams contributing to the one meson-loop gap equation (39). The dashed line corresponds to the meson propagator \widetilde{K} defined in Eq. 41, the solid circle corresponds to the quark loop, and the filled quark-loop meson vertex is defined in App. A (see Fig. 11). Diagram (a) corresponds to the quark-loop contribution and diagram (b) to the meson-loop contribution. The cross denotes the constant term a^2 .

$$\begin{array}{ccccccc}
 \mathbf{L}^{-1} = & \text{a} & - \frac{1}{2} & \text{b} & + \frac{1}{2} & \text{c}
 \end{array}$$

Fig. 2. Diagrams contributing to the inverse meson propagator in one meson-loop approximation. The dashed line corresponds to the meson propagator \widetilde{K} , and the filled quark-loop meson vertices are defined in App. A (see Figs. 11, 12).

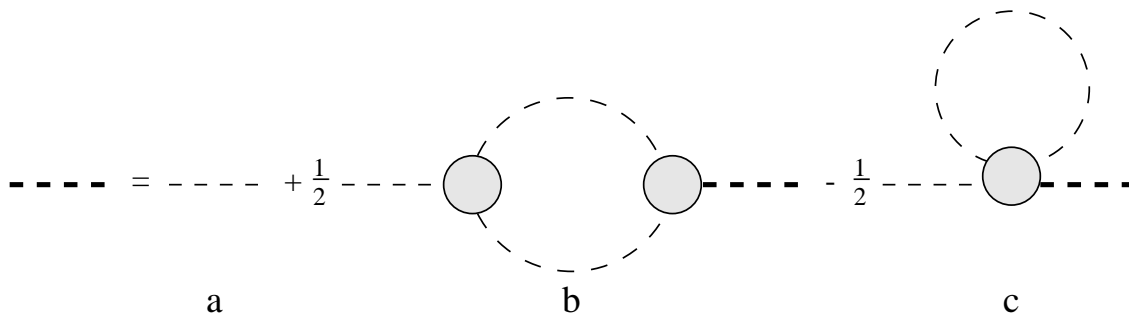


Fig. 3. The meson propagator in one meson-loop approximation. The thick dashed lines correspond to the meson propagator L with the meson loop included, the thin external dashed lines—to the leading-order fermion-loop meson propagator K , and the dashed lines in the loops—to \widetilde{K} . The filled quark-loop meson vertices are defined in App. A.

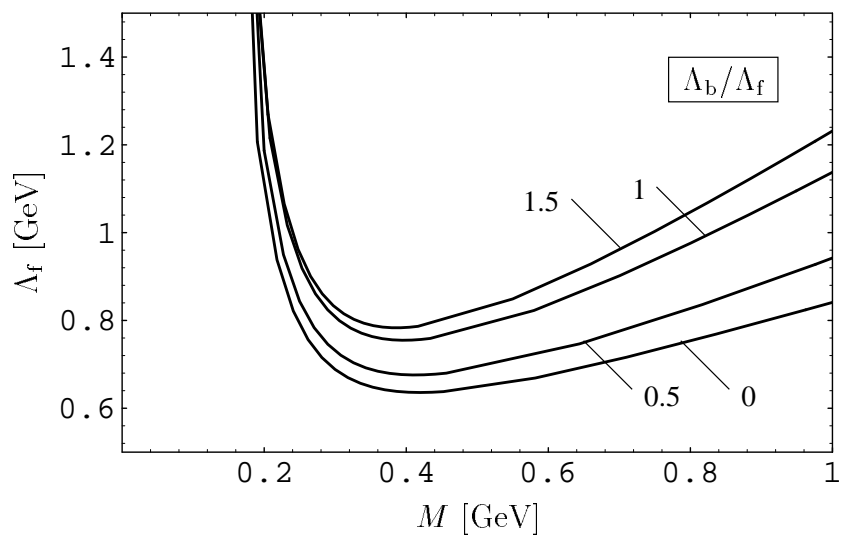


Fig. 4. The fermionic cut-off Λ_f for proper-time quark-loop regularization as a function of the constituent quark mass M for different values of Λ_b/Λ_f . The curves correspond to $\Lambda_b/\Lambda_f = 0, 0.5, 1, 1.5$.

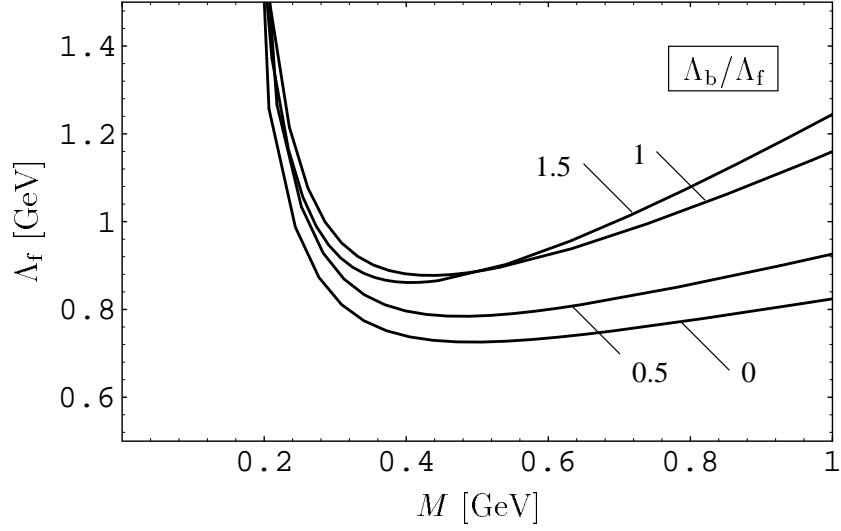


Fig. 5. The fermionic cut-off Λ_f for $O(4)$ quark-loop regularization as a function of the constituent quark mass M for different values of Λ_b/Λ_f . The curves correspond to $\Lambda_b/\Lambda_f = 0, 0.5, 1, 1.5$. Note that the curve for $\Lambda_b/\Lambda_f = 1.5$ has the critical Λ_f smaller than for $\Lambda_b/\Lambda_f = 1$.

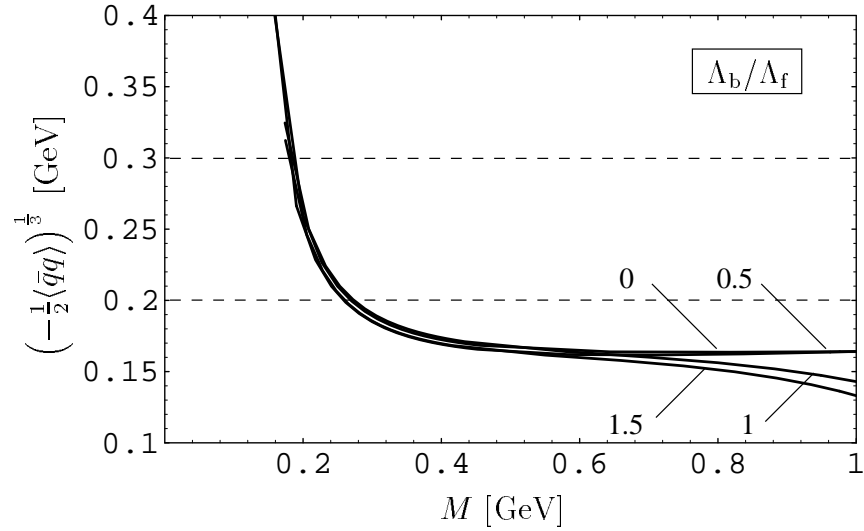


Fig. 6. The quark condensate $\left(-\frac{1}{2}\langle\bar{q}q\rangle\right)^{\frac{1}{3}}$ with proper-time quark-loop regularization as a function of M for different values of Λ_b/Λ_f . The curves correspond to $\Lambda_b/\Lambda_f = 0, 0.5, 1, 1.5$. The dashed lines mark the empirical bounds.

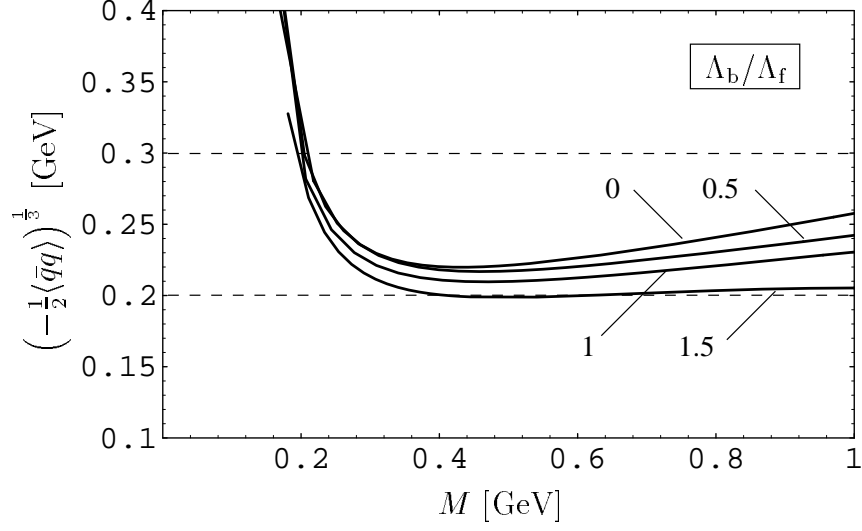


Fig. 7. The quark condensate $\left(-\frac{1}{2}\langle\bar{q}q\rangle\right)^{\frac{1}{3}}$ with $O(4)$ quark-loop regularization as a function of M for different values of Λ_b/Λ_f . The curves correspond to $\Lambda_b/\Lambda_f = 0, 0.5, 1.5, 1$. The dashed lines mark the empirical bounds.

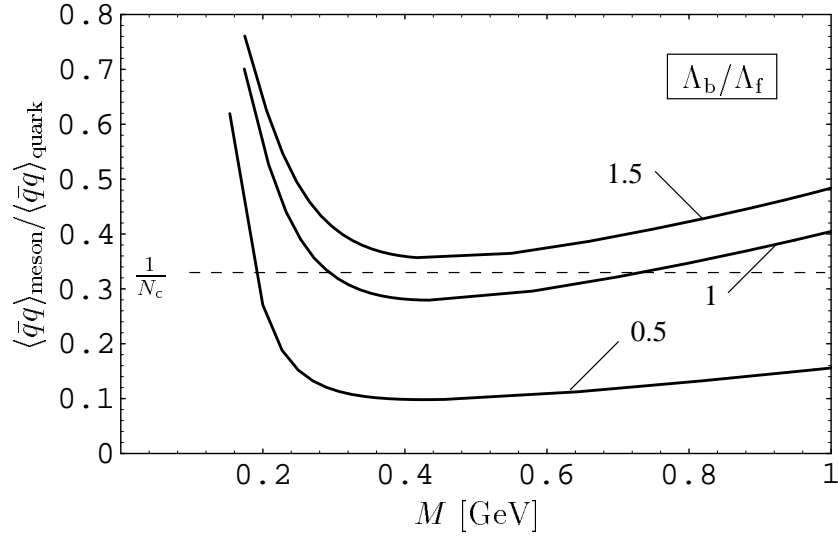


Fig. 8. The ratio of the meson-loop to the quark-loop contribution to $\langle\bar{q}q\rangle$ as a function of M obtained with proper-time fermion-loop regularization. The curves correspond to $\Lambda_b/\Lambda_f = 0.5, 1, 1.5$.

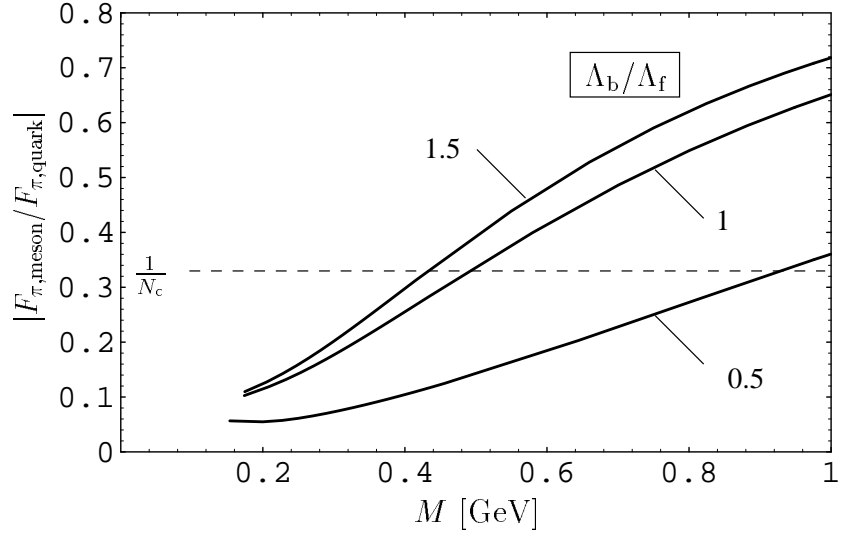


Fig. 9. The ratio of the meson-loop to the quark-loop contribution to F_π as a function of M obtained with proper-time fermion-loop regularization. The curves correspond to $\Lambda_b/\Lambda_f = 0.5, 1, 1.5$.

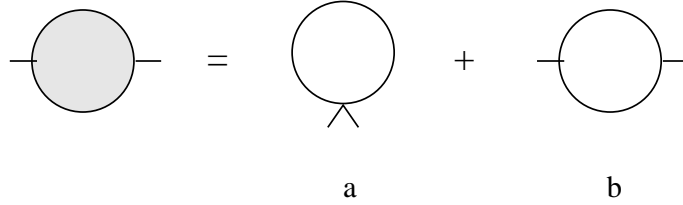


Fig. 10. The two-leg quark-loop vertex (A.8). The diagrams a and b correspond to the terms proportional to the functions g and f respectively.

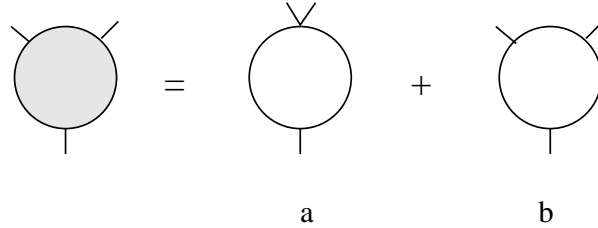


Fig. 11. The three-leg quark-loop vertex (A.14). The diagrams a and b correspond to the contributions $S_{abc}^{(A)}$ and $S_{abc}^{(B)}$.

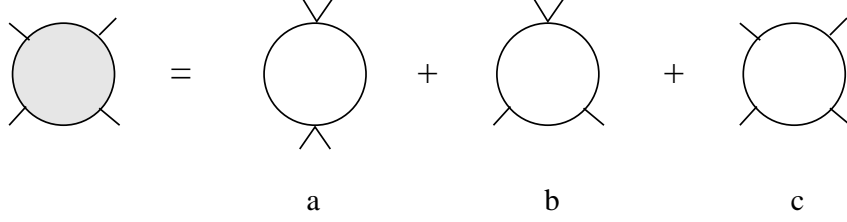


Fig. 12. The four-leg quark-loop vertex (A.23). The diagrams a , b and c correspond to the contributions $S_{abcd}^{(A)}$, $S_{abcd}^{(B)}$ and $S_{abcd}^{(C)}$.

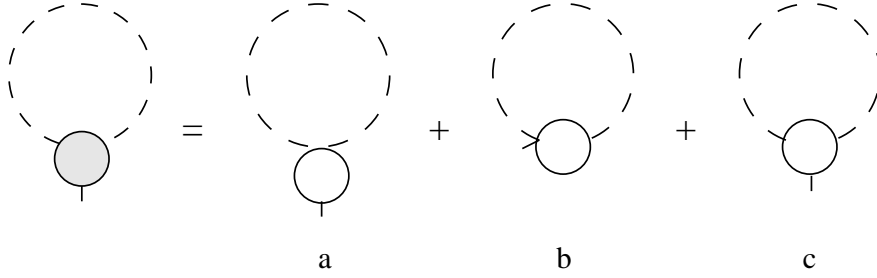


Fig. 13. The meson-loop contributions to the one meson-loop gap equation.

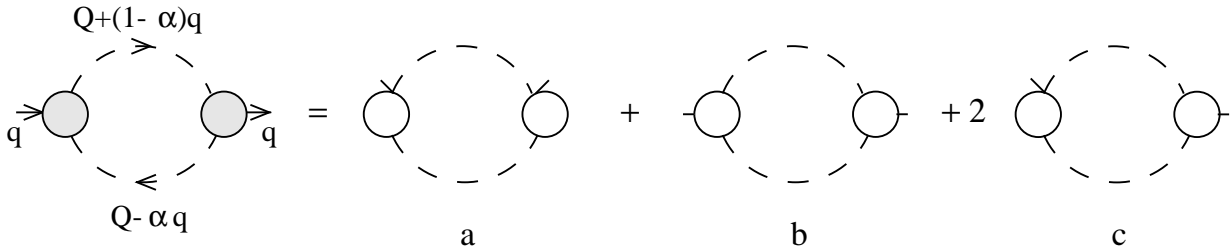


Fig. 14. The meson-loop contributions of diagram (b) in Fig. 2 to the inverse pion propagator.

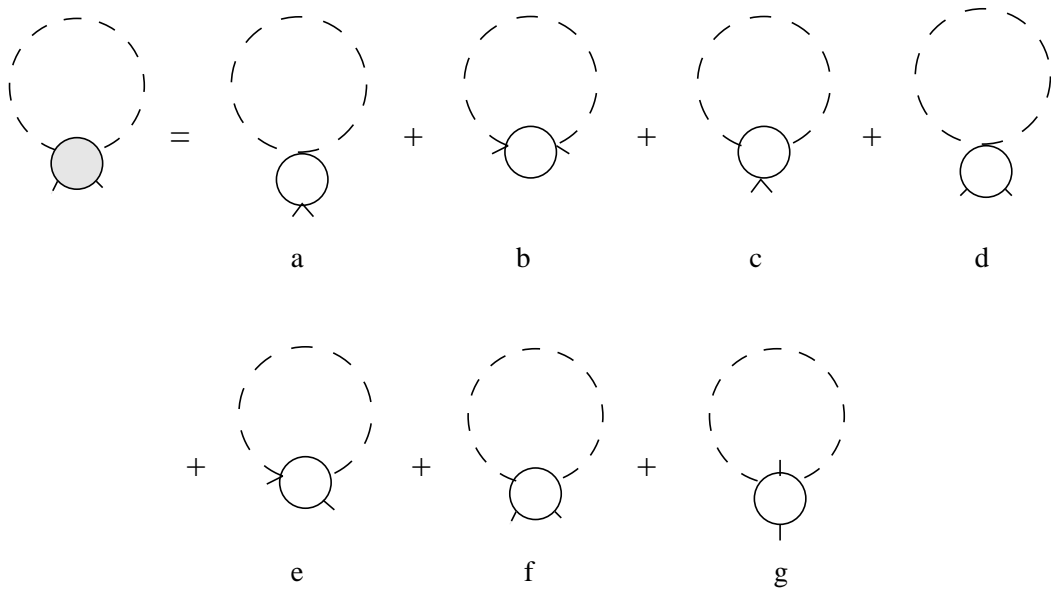


Fig. 15. The meson-loop contributions of diagram (c) in Fig. 2 to the inverse pion propagator.